Physics – Uspekhi **43** (9) 901 – 920 (2000)

REVIEWS OF TOPICAL PROBLEMS PACS numbers: **36.40.–c**, 52.40.Nk, **61.46.+w**, **85.42.+m**

The evolution of large clusters under the action of ultrashort superintense laser pulses

V P Kraĭnov, M B Smirnov

DOI: 10.1070/PU2000v043n09ABEH000803

Contents

Abstract. **The evolution of large clusters exposed to a superintense ultrashort laser pulse is considered. Cluster excitation results from the interaction of its electron subsystem with the laser field. Multiple ionization and X-ray emission followed by explosion in clusters irradiated by a laser field are investigated. The increase of the electron temperature in this process and of the charge of the cluster ion are discussed. The reabsorption of photons in such a plasma is found to be relatively small. The optimal conditions are analyzed for efficient absorption of laser radiation by large clusters. This absorption occurs on the surface of the cluster only. The review is done of the works devoted to X-ray emission and generation of high harmonics of the incident radiation from a hot cluster ion. The optical density of the cluster plasma is found to be relatively small for resonance photons of multiply charged atomic ions produced inside the cluster. Expansion and decay of the cluster during and after the laser pulse are discussed.**

V P Kraĭnov Moscow Institute of Physics and Technology, 141700 Dolgoprudnyĭ, Moscow Region, Russian Federation
E-mail: krainov@cyberax.ru
M B Smirnov Max-Born Institute, Abt. B2, Rudower Chaussee 6, 12489 Berlin, Germany,
Russian Research Center 'Kurchatov Institute', pl. Kurchatova 1, 123182 Moscow, Russian Federation
E-mail: smirnov@mbi-berlin.de

Received 24 May 2000
Uspekhi Fizicheskikh Nauk **170** (9) 969 – 990 (2000)
Translated by A S Dobroslavskiĭ; edited by A Radzig

1. Introduction

The exposure of large clusters comprising several thousand atoms or molecules to the field of an ultrashort superintense laser pulse (about a hundred femtoseconds long or some 30 periods of laser field) produces highly excited matter [1, 2]. The heating of conduction electrons in the case of metal clusters (or primary ionized electrons in the case of clusters of inert gas atoms) on the one hand, and the absence of a fast heat sink mechanism like that in an ordinary plasma on the other, allow the achievement of a state of much greater excitation of the electron subsystem as compared with the excitation of isolated atoms and molecules. In this case atomic ions remain practically unheated. Following the fast initial multiple ionization, for the rest of the duration of the laser pulse, the matter of the cluster ion is an ideal plasma composed of electrons and multiply charged atomic ions. The evolution of a cluster in a laser field was studied both experimentally [3, 4] and theoretically [5, 6] using a variety of numerical and analytical methods.

We shall consider models of cluster plasma that allow analysis of the properties of this system in the course of generation of dense plasma with a laser pulse. These models describe heating of the cluster, when the mean energy of the electron (that is, the electron temperature T) increases to a few keV. Then collision processes become very important. Electron – electron collisions may result in a Maxwellian distribution with a certain relation between the mean thermal energy of electrons, $3T/2$, and their mean vibrational energy $U_p = F^2/4\omega^2$ in laser field, with the former quantity being either greater or smaller than the latter. Notice

that here and further we shall use, as a rule, the Hartree atomic units: $m_e = e = \hbar = 1$. The electron temperature T increases until the expansion of cluster ion becomes significant.

Exposure to a laser pulse, apart from heating the electrons, leads to some of the electrons leaving the cluster, either forced out by the field of the laser pulse itself or by thermal evaporation from the cluster surface. Accordingly, the charge Z' of the cluster ion increases throughout the duration of the laser pulse. Later we shall give a simple relationship between the growth of the electron temperature T and the cluster ion charge Z'.

Straightforward estimates confirm that the cluster plasma is ideal. The condition of ideality is written as

$$NZ^3 \ll T^3 ,$$

where N is the concentration of atoms in the cluster, Z is the mean charge of an atomic ion within the cluster (not to be confused with the cluster charge Z'!), and T is the electron temperature. When the electron temperature is high, this inequality is usually satisfied, notwithstanding the high density of cluster plasma (including metal clusters, whose density is the same as that of liquid metal; see Table 1). For example, for clusters of sodium atoms ($Z = 11$ when the atom is completely stripped) and $T = 1$ keV we have $NZ^3/T^3 \sim 10^{-4}$.

Excited multiply charged atomic ions within the cluster emit X-radiation. We shall demonstrate that the share of this radiation in the energy balance of a cluster in the heating is negligible. The power of radiation emitted by a cluster is calculated. However, spontaneous and induced transitions in multiply charged ions occur within times that decrease quickly as the charge of the atomic ion increases. These processes may considerably change the balance between the atomic ions in a cluster. Therefore, an important role in such a system may belong to the resonant reabsorption of this radiation by other atomic ions within the cluster, which affects the time of radiation transition. We shall study this role as well.

2. Staging of experiments

Let us discuss the typical experimental setups used for studying the interaction of clusters with short powerful laser pulses. Most of the experiments were carried out with clusters of atoms of inert (rare) gases or simple diatomic molecules. The number of particles in the cluster varied up to one million. Some experiments were done with metallic clusters containing from a few to a thousand particles. The size of clusters depended on the technique used for their production.

Let us describe here the methods of generation and measurement of clusters of inert gas atoms. The typical experimental installation is represented schematically in Fig. 1. The cluster beam is formed as the gas expands during its flow through a supersonic nozzle into vacuum. The diameter of the nozzle is about 0.5 cm. The gas upstream of the nozzle was maintained at a controllable pressure of several tens of atmospheres and room temperature, and passed through the nozzle into the high-vacuum chamber. The quasi-stationary nuclei in the supersonic gas jet were removed in front of the high-vacuum chamber by means of the skimmer a few millimeters in diameter (in some experiments the skimmer was not used). The feasibility of cluster formation from atoms depends on the value of the empirical

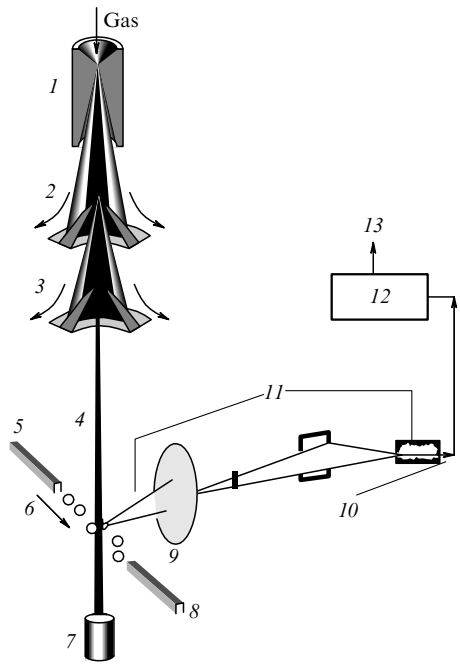

Figure 1. Typical experimental configuration for production and measurement of clusters: *1* — nozzle, *2* — skimmer, *3* — collimator, *4* — cluster beam, *5* — cathode, *6* — electron beam, *7* — Faraday cage, *8* — anode, *9* — slit, *10* — X-ray spectrograph, *11* — X-rays, *12* — amplifier, *13* — data processing.

dimensionless Hagena parameter [7, 8]

$$\Gamma = k\left(\frac{d}{\tan\alpha}\right)^{0.85} \frac{p}{T_0^{2.29}} .$$

Here d is the diameter of the critical cross section of the supersonic nozzle measured in μm, 2α is the flare angle of the nozzle, p is the pressure in mbar, k is the empirical coefficient different for diverse atoms (for example, $k = 2900$ for krypton, and $k = 180$ for neon). Finally, T_0 is the initial temperature of the gas. Clustering starts when the Hagena parameter is $\Gamma > 300$ [9, 10]. For $\Gamma > 50{,}000$ each cluster contains as many as 10,000 atoms and more.

The diameter of the outgoing cluster beam is from 0.5 to 2.0 cm. Measurements of clusters were made leaning upon Rayleigh scattering. The range of powers and wavelengths of laser radiation used in the experiments is very wide: from 10^{15} to 10^{20} W cm^{-2}, and from 248 to 800 nm, respectively. The duration of the laser pulse varied from several tens of femtoseconds to tens of picoseconds.

The first series of experiments was carried out by the Rhodes team [11, 12]. They used laser radiation with a peak intensity from 10^{16} to 10^{20} W cm^{-2}, a wavelength of 248 nm, and a pulse length of about 270 fs. The focal diameter was about 0.3 mm. Laser radiation was focused in the region of clustering 2 mm below the exhaust valve (no skimmer). The number of particles in the cluster ranged up to about 30. Clusters were made up of atoms of inert gases: xenon, krypton, and argon.

Similar experiments were carried out with an alternative source of laser radiation with an intensity of 10^{18} W cm^{-2}, a wavelength of 800 nm, and a pulse length of 90 fs [13, 14]. The focal diameter was about 0.6 mm. The main purpose of the experiments consisted in studying the X-rays generated (see

Section 7) by the radiative transitions in multiply charged atomic ions in the clusters. The possible use of UV and visible laser radiation for producing high-power X-ray emission was discussed (see also Ref. [15]).

The next group of experiments [5, 6] is distinguished by its especially deep treatment. Clusters made up of xenon and krypton atoms, and of CO_2 molecules were studied. The results include the energy spectra of ionization electrons and atomic ions, data on the generation of harmonics, and the efficiency of laser radiation absorption by clusters. The length of the laser pulse comprised about 1 ps, the wavelength 800 nm, and the peak intensity from 10^{15} to 10^{17} W cm^{-2}. The clusters contained from 10^3 to 10^6 atoms. The fraction of atoms building up clusters in the gas jet was as large as 10%. The region of interaction of the laser beam with the clusters was situated 20 cm downstream of the exhaust valve, and measured about 1 mm.

The main attention in Refs [16, 17] was focused on measuring the energy spectra of ions after the explosion of a cluster, and on the X-ray emission spectra. Like in the previous set of experiments, the region of interaction was removed from the nozzle, but the parameters of the laser pulse were much different. First, a neodymium laser was used with a wavelength of 1064 nm, a pulse length of 30 ps, and an intensity of about 10^{14} W cm^{-2}. Then the experiments were done with a titanium–sapphire laser (wavelength 790 nm), with the pulse length varying from 60 to 200 fs, and the peak intensity ranging from 10^{16} to 10^{18} W cm^{-2}.

A number of experimental works [18–20] dealt with the interaction of metal clusters with high-intensity laser radiation. The lasers had intensities up to 10^{16} W cm^{-2}, a wavelength of 800 nm, and pulse lengths from 100 fs to 1 ps. The number of particles in the cluster varied from 20 to 1000; clusters were made up of atoms of platinum, silver and lead. The yield of multiply charged ions as a function of the length of a laser pulse was measured, while the energy of the pulse was kept constant. The yield exhibited a maximum at a certain pulse length.

3. Properties of metal clusters

One of the key topics of this review is the evolution of large metal clusters in the field of a superintense laser pulse. The main properties of such clusters are described in the reviews [21–25]. In metal clusters, like in common liquid metal, the valence electrons are to a large extent delocalized. In the case of alkaline elements, the only valence s electron is completely delocalized. The description of the structure of large metallic clusters, as a rule, is based on the so-called *jellium model*. In this model, the cluster is a spherical liquid drop (whose size is small compared with the wavelength of laser radiation) which has a sharp surface boundary for positive ions. The ions are uniformly distributed in the bulk of the cluster. The cloud of conduction electrons goes slightly beyond this boundary, the less so the bigger the cluster. As already indicated, the electron gas in the cluster may be quite safely regarded as ideal. Accordingly, one may apply the known bulk and surface parameters of liquid metals to a large cluster. Of course, such an approach does not allow the description, for example, of properties related to the shell structure of small clusters.

Let R be the radius of cluster in such a model of a liquid drop. The ionization potential of a large neutral cluster equals the work function W for the corresponding metal. If we are dealing with a cluster ion with the charge $Z' \gg 1$, then to the work function we must add the Coulomb energy of the electron detachment. Assuming the excess charge Z' of the cluster ion is distributed over the surface of the cluster, this energy equals Z'/R (see the review [22]). Then the ionization potential $J_{Z'}$ of the cluster ion is given by a simple relation

$$J_{Z'} = W + \frac{Z'}{R}$$

(observe that when Z' is rather small, ~ 1, the Coulomb energy is different from this estimate. For example, the Coulomb energy for the charge $Z' = 1$, distributed over the surface of the cluster ion, amounts to $1/2R$).

By assumption (which will be verified later), the fraction of escaping electrons is small, i.e.

$$Z' \ll n' ,$$

where n' is the total number of free electrons inside the cluster. In addition, in the framework of the model of a liquid drop we suppose that the cluster density is the same as that of liquid metal. Therefore, the radius of the cluster is

$$R = r_W n^{1/3} ,$$

where r_W is the *Wigner–Seitz radius*, and n is the number of atoms in the cluster. At the beginning of the laser pulse, this number coincides with the number of conduction electrons n' (for alkali atoms). In the course of the laser pulse, the number of free electrons n' grows considerably because of the internal ionization of atoms in the cluster.

The Wigner–Seitz radius in the drop model can be expressed in terms of the density ρ of liquid metal and mass M of an individual atom:

$$r_W = \left(\frac{3M}{4\pi\rho}\right)^{1/3} = \left(\frac{3}{4\pi N}\right)^{1/3} .$$

Here N is the atomic concentration in the cluster.

Table 1 presents the values of the work function W, the Wigner–Seitz radius r_W, the concentration of atoms N, and the Fermi energy E_F of valence electrons for a number of univalent metals at melting point.

Table 1. Basic parameters of liquid metals, used for description of clusters [26, 27].

Metal	Z	N, 10^{22} cm^{-3}	E_F, eV	r_W, Å	$1/(r_W E_F)$	W, eV
Li	3	4.44	4.72	1.75	1.8	2.9
Na	11	2.44	3.23	2.14	2.2	2.75
Al	13	5.33	11.63	1.65	0.75	4.28
K	19	1.27	2.12	2.65	2.7	2.30
Cu	29	7.50	7.00	1.47	1.4	4.65
Mo	42	5.86	8.73	1.60	1.0	4.6
Ag	47	5.20	5.48	1.66	1.6	4.26
Cs	55	0.84	1.58	3.05	3.1	2.14
W	74	5.80	8.67	1.60	1.0	4.55
Au	79	5.29	5.51	1.65	1.6	5.1

From Table 1 it follows that the Coulomb electrostatic energy $1/r_W$ of interaction of nearest neighboring electrons with one another is comparable with the Fermi energy for conduction electrons. Accordingly, the exchange interaction which is responsible for the establishment of the Fermi level

and the direct Coulomb interaction between electrons are of the same order of magnitude. Because of this, the electrons in the cold cluster form an essentially quantum subsystem. However, the role of exchange effects decreases as the charge of the cluster ion and the concentration of free electrons both increase.

4. Structure of large clusters

4.1 Cold clusters and cluster ions

Kresin [21] proposed using the numerical Thomas – Fermi model for the description of the quantum-mechanical electron distribution in cold metallic clusters ($T = 0$). This model does not reflect the shell properties of small clusters. The dynamics of interacting electrons are most commonly described with the Kohn – Sham mean field model [22, 23]. This model is validated by the theory of time-dependent density functional [24, 28], whereby the calculations are carried out in the approximation of time-dependent local density [29]. It is also employed for analyzing the collisions of clusters with high-energy ions using the quasi-classical representation of the electron subsystem, based on the Vlasov equations [30, 31]. The emission of electrons by metallic clusters for processes of fast excitation is considered in Ref. [32].

4.1.1 Neutral clusters. We start with the description of large spherical cold neutral clusters ($T = 0$). In this case the Thomas – Fermi model can be simplified [33, 34]. The jellium model mentioned above gives the distribution of positive ions. We denote the radius of the ion sphere by R, and the number of atoms in the cluster (or ions in the case of univalent metallic clusters) by $n \gg 1$. The Poisson equation for the electrostatic potential $\varphi(r)$ for $r < R$ — that is, within the ion sphere — is written (recall once again that we are using the system of Hartree atomic units, $m_e = e = \hbar = 1$) as

$$\Delta\varphi = \frac{d^2\varphi}{dr^2} + \frac{2}{r}\frac{d\varphi}{dr} = \frac{4}{3\pi}(2\varphi)^{3/2} - \frac{3n}{R^3}\,. \tag{1}$$

Throughout most of the ion sphere (with the exception of narrow region beneath the surface) this potential is constant, $\varphi = \varphi_0$. Accordingly, there is no electric field here. The constant φ_0 can be found from Eqn (1) by equating the right-hand side to zero:

$$\varphi_0 = \frac{(9\pi n)^{2/3}}{2^{7/2}R^2} = \frac{(9\pi)^{2/3}}{2^{7/2}r_W^2}\,, \tag{2}$$

since $R = r_W n^{1/3}$, with the Wigner – Seitz radius r_W being equal to about 1 a.u. (see Table 1). Hence, the value of the potential φ_0 is also of the order of 1 a.u. For example, for a cluster of sodium atoms we get $\varphi_0 = 3.1$ eV.

Now we seek the solution of Eqn (1) with $r < R$ in the form

$$\varphi(r) = \varphi_0\left[1 - a\left(\frac{r}{R}\right)^k\right]. \tag{3}$$

Here $a \sim 1$ and $k \gg 1$ are the constants whose values will be deduced shortly. Note that this solution differs from a constant φ_0 only near the surface of the cluster. Substituting solution (3) into Eqn (1) and taking Eqn (2) into account, we find the value of constant k:

$$k^2 = \left(\frac{3}{\pi^2}\right)^{2/3} Rn^{1/3} \approx 0.452Rn^{1/3} \gg 1\,. \tag{4}$$

The electron cloud goes slightly beyond the ion sphere. We seek a diminishing solution for the electrostatic potential φ at $r > R$ in the form

$$\varphi(r) = \varphi_0 b\left(\frac{R}{r}\right)^l. \tag{5}$$

Here $b \sim 1$ and $l \gg 1$ are the constants which will be defined below.

Matching the potentials (3) and (5) together with their derivatives at $r = R$ gives us two equations for finding the constants:

$$a + b = 1\,, \qquad ak = bl\,. \tag{6}$$

The additional equation follows from the condition that the number of electrons in a neutral cluster equals the number of ions n:

$$n = \frac{1}{3\pi^2}\int_0^\infty (2\varphi)^{3/2} r^2\,dr\,. \tag{7}$$

Substituting Eqns (3) and (5) into (7), we expand the integrand in a Taylor series for $r < R$:

$$n = \frac{(2\varphi_0)^{3/2}}{3\pi^2}\left\{\int_0^R\left[1 - \frac{3a}{2}\left(\frac{r}{R}\right)^k\right]r^2\,dr + \int_R^\infty b^{3/2}\left(\frac{R}{r}\right)^{3l/2} r^2\,dr\right\}. \tag{8}$$

Taking the simple integrals and using Eqn (2) and inequalities $k, l \gg 1$, we rewrite this equation in the following form

$$9al = 4b^{3/2}k\,. \tag{9}$$

From Eqns (6) and (9) it follows that the constant a is found from the solution of the transcendental equation

$$a + \left(\frac{9a^2}{4}\right)^{2/5} = 1\,. \tag{10}$$

Solving this equation, we find the universal values of the constants $a = 0.372$ and, according to Eqn (9), $b = 0.628$.

To calculate the characteristic values of constants k and l, we consider a typical example of a cluster of $n = 10^5$ sodium atoms. For this purpose we use the data from Table 1: a Wigner – Seitz radius $r_W = 2.14$ Å, and a cluster radius $R = r_W n^{1/3} = 99$ Å $= 188$ a.u. According to Eqn (4), we find that $k = 62.77$, and from Eqn (6) one gets $l = 37.16$. Thus, we may conclude that the distribution of electrons very closely follows a stepwise pattern, and is practically the same as the distribution of ions.

Indeed, the difference between the electrostatic potential φ inside the cluster and the constant φ_0 is only significant within a small distance δ from the cluster surface. According to Eqn (3), we have

$$\delta = R - r \sim \frac{R}{k} = \frac{R}{63} \ll R\,.$$

Outside the ion sphere, the electron concentration rapidly decreases. The distance δ', at which the potential $\varphi(r)$ declines practically to zero, can be found from Eqn (5):

$$\delta' = r - R \sim \frac{R}{l} = \frac{R}{37} \ll R .$$

When the number of particles is large, the Thomas–Fermi model becomes the model of a liquid drop with a sharp boundary.

4.1.2 Cluster ions. Let us consider a cold cluster ion with the charge Z'. Solutions (3) and (5) keep the same form, but the constants are different. The number of electrons is now $n - Z'$, and the condition (8) is replaced by

$$n - Z' = \frac{(2\varphi_0)^{3/2}}{3\pi^2} \left\{ \int_0^R \left[1 - \frac{3a}{2} \left(\frac{r}{R} \right)^k \right] r^2 \, \mathrm{d}r + \int_R^\infty b^{3/2} \left(\frac{R}{r} \right)^{3l/2} r^2 \, \mathrm{d}r \right\} .$$

Taking the integrals, in place of Eqn (9) we get the equation

$$9al = 4b^{3/2}k + 2kl \frac{Z'}{n} , \tag{11}$$

which must be solved jointly with Eqn (6). Eliminating b and l, we arrive at the transcendental equation for finding the constant a [in place of Eqn (10)]:

$$a + \left(\frac{9a^2}{4} - \frac{Z'ak}{2n} \right)^{2/5} = 1 . \tag{12}$$

We consider the same example of a cluster of $n = 10^5$ sodium atoms, but the degree of ionization of the cluster ion this time is $Z'/n = 0.05$. According to Eqn (4), we again have $k = 62.77$. Then from Eqn (12) it follows that $a = 0.723$. Accordingly, $b = 0.277$ and $l = 164$. We see that the 'tail' of electron concentration outside the cluster is much smaller compared to a neutral cluster with the same number of atoms. From Eqn (12) it also follows that the electron 'tail' outside the cluster disappears at a certain (relatively small) degree of ionization of the cluster ion $Z'/n = 0.07$ altogether. Then $a = 1$, and $b = 0$.

On the whole, one may conclude that the electron 'tail' outside the cluster decreases with increasing number of atoms n in the cluster and with increasing charge Z' of the cluster ion.

4.1.3 Time-dependent Thomas–Fermi approximation. The time-dependent Thomas–Fermi approximation as applied to three-dimensional cluster dynamics was developed in Ref. [35]. We shall discuss a simplified version of this approximation.

Consider natural oscillations of the electron cloud within the cluster. We use the same method as was applied in Ref. [36] when calculating the static polarizability of atoms and ions in the Thomas–Fermi approximation. We define a small monochromatic perturbation of the electric potential $\varphi \to \varphi_0 + \delta\varphi$, $\delta\varphi \ll \varphi_0$. Then the first iteration of the Thomas–Fermi equation (1) for $r < R$ becomes

$$\Delta\delta\varphi = \frac{4}{\pi\varepsilon} \sqrt{2\varphi_0} \, \delta\varphi . \tag{13}$$

Here

$$\varepsilon = 1 - \left(\frac{\omega_\mathrm{p}}{\Omega} \right)^2 < 0 \tag{14}$$

is the dielectric constant created by free electrons of the cluster, and Ω is the eigen-frequency. The plasma frequency ω_p is given by the known relation (here we assume that the field of laser radiation is homogeneous throughout the entire cluster)

$$\omega_\mathrm{p} = \sqrt{4\pi N_\mathrm{e}} ,$$

where N_e is the electron concentration.

Observe that the appearance of the permittivity of the cluster in the electrostatic Poisson equation (13), in contrast to Eqn (1), is due to the fact that the quantity $\delta\varphi(r, t)$ is treated as an external perturbation with respect to the stationary distribution of charges in the cluster, which imparts dielectric properties to the material of the cluster.

Introducing the notation

$$k^2 = -\frac{4}{\pi\varepsilon} \sqrt{2\varphi_0} > 0 , \tag{15}$$

we rewrite Eqn (13) in spherical coordinates for $r < R$:

$$\frac{\partial^2 \delta\varphi}{\partial r^2} + \frac{2}{r} \frac{\partial \delta\varphi}{\partial r} + \frac{1}{r^2 \sin\theta} \frac{\partial}{\partial\theta} \left(\sin\theta \frac{\partial \delta\varphi}{\partial\theta} \right) = -k^2 \delta\varphi . \tag{16}$$

The solution of this equation is sought in the form of dipole oscillations (for $r < R$):

$$\delta\varphi(r, t) = u(r) \cos\theta \cos\Omega t . \tag{17}$$

Substituting Eqn (17) into (16), we get the ordinary differential equation in the function $u(r)$:

$$\frac{\mathrm{d}^2 u}{\mathrm{d}r^2} + \frac{2}{r} \frac{\mathrm{d}u}{\mathrm{d}r} - \frac{2u}{r^2} = -k^2 u . \tag{18}$$

Its solution, regular at the origin of the coordinates, has a simple analytical form

$$u(r) = A \left(\frac{\sin kr}{kr^2} - \frac{\cos kr}{r} \right) , \qquad r < R . \tag{19}$$

Here A is an arbitrary constant that defines the amplitude of natural oscillations.

Now we find the solution outside the ion sphere (for $r > R$). The dipole solution of Laplace equation

$$\frac{\partial^2 \delta\varphi}{\partial r^2} + \frac{2}{r} \frac{\partial \delta\varphi}{\partial r} + \frac{1}{r^2 \sin\theta} \frac{\partial}{\partial\theta} \left(\sin\theta \frac{\partial \delta\varphi}{\partial\theta} \right) = 0 , \tag{20}$$

regular at infinity, takes the form

$$\delta\varphi(r, t) = \frac{B}{r^2} \cos\theta \cos\Omega t . \tag{21}$$

Here B is also a constant.

The potential $\delta\varphi$ must be continuous at the boundary of the ion sphere, $r = R$. From Eqns (19) and (21) it follows that

$$A \left(\frac{\sin kR}{kR^2} - \frac{\cos kR}{R} \right) = \frac{B}{R^2} . \tag{22}$$

The second boundary condition requires continuity of the normal projection of electric displacement vector at $r = R$ — that is, one obtains

$$A\varepsilon \frac{\mathrm{d}}{\mathrm{d}r}\left(\frac{\sin kr}{kr^2} - \frac{\cos kr}{r}\right)_{r=R} = -B\,\frac{2}{R^3}\,. \tag{23}$$

Dividing Eqn (23) by Eqn (22) term by term, we eliminate the constants A and B. This gives us the implicit relationship for the eigen-frequency Ω of dipole oscillations of the cluster electron cloud in the Thomas – Fermi approximation:

$$\Omega = \omega_{\mathrm{p}}\sqrt{1 + \frac{2(kR\cot kR - 1)}{(kR)^2}}\,. \tag{24}$$

In the limit of a very small cluster $kR \ll 1$, from Eqn (24) we get

$$\Omega = \frac{\omega_{\mathrm{p}}}{\sqrt{3}}\,, \tag{25}$$

which is the well-known Mie frequency of surface dipole oscillations of a small (compared with the wavelength c/Ω) metallic sphere. From Eqn (24) it follows that, as the radius R increases, the frequency of natural oscillations decreases in comparison with the Mie frequency. In the opposite limit of a very large cluster ($kR \gg 1$), after some algebra from Eqn (24) we find

$$\Omega = \frac{\omega_{\mathrm{p}}}{\sqrt{1 + 0.31(R/l)^2}}\,. \tag{26}$$

Here we introduced the so-called *Thomas – Fermi screening length*

$$l = (2\varphi_0)^{-1/4}\,.$$

If $R/l \ll 1$, then from Eqn (19) it follows that $u(r) \sim r$ for $r < R$. Thus, in this limit the quantum screening is absent, and the electric field strength inside the cluster is uniform. This is the classical surface dipole oscillations of an electron cloud as a whole (without change of density) at the Mie frequency (similar to Goldhaber – Teller oscillations in the case of nuclear dipole resonance). Solutions (19), (21) in this limit coincide with the solution obtained in the classical random phase approximation [21]. The Thomas – Fermi screening is important when $R/l > 1$. Obviously, it cannot be obtained in the classical random phase approximation [21].

Equation (24) also admits a trivial solution $\Omega = \omega_{\mathrm{p}}$ ($k^2R^2 \to -\infty$), which corresponds to classical bulk plasma oscillations (with density variations). Similar oscillations known as Steinwedel – Jensen oscillations in atomic nuclei are only realized in superheavy elements.

Observe that in the case of a stepwise distribution of electron concentration, the classical random phase approximation [21] yields two frequencies: $\Omega = \omega_{\mathrm{p}}/\sqrt{3}$ and $\Omega = \omega_{\mathrm{p}}$. However, the dynamic polarizability of a cluster for a stepwise electron concentration distribution does not exhibit a resonance at $\Omega = \omega_{\mathrm{p}}$, because the corresponding oscillator strength is zero [21]. According to our quantum approach, based on the Thomas – Fermi approximation, there also are two modes, but the lower frequency decreases with respect to the Mie frequency $\Omega = \omega_{\mathrm{p}}/\sqrt{3}$ as the size of the cluster increases, because of the effect of Thomas – Fermi screening.

Consider a typical example of a cluster of $n = 40$ sodium atoms. In this case $R/l = 9.5 \gg 1$. From Eqn (24) it follows that $\Omega = 0.18\omega_{\mathrm{p}}$. Thus, the frequency of natural oscillations of metallic clusters is lower than the Mie frequency $\Omega = \omega_{\mathrm{p}}/\sqrt{3}$. For sodium, the plasma frequency equals $\omega_{\mathrm{p}} = 5.80$ eV, and therefore $\Omega = 1$ eV. The true value of the eigen-frequency, examined experimentally, is somewhat higher. This is attributed to the fact that the calculations disregarded the electron distribution diffusivity. The diffusive boundary of the electron cloud weakens the effect of Thomas – Fermi screening. Taking the diffusivity into account is only possible with numerical calculations.

So we may conclude that the quantum metallic cluster is essentially different from a small metallic sphere: the eigen-frequency of surface oscillations of the cluster is lower than the Mie frequency because of Thomas – Fermi screening.

4.1.4 Dynamic polarizability of a cluster. In the preceding section we looked into the natural dipole surface oscillations of the electron cloud in a metallic cluster. Now we shall consider induced dipole oscillations caused by the external electromagnetic (laser) field of strength $F\cos\omega t$. In place of Eqn (21), the solution of differential equation (20) outside the ion sphere (for $r > R$) takes the form

$$\delta\varphi = F\left[-r + \frac{\alpha(\omega)}{r^2}\right]\cos\theta\cos\omega t\,, \tag{27}$$

where $\alpha(\omega)$ is the dynamic polarizability of the cluster.

The solution of Eqn (16) is similar to solution (19), but this time with a fixed constant A and with the replacement $\Omega \to \omega$:

$$\delta\varphi = A\left(\frac{\sin kr}{kr^2} - \frac{\cos kr}{r}\right)\cos\theta\cos\omega t\,.$$

According to (15) we have

$$k^2 = \frac{4\omega^2}{\pi(\omega_{\mathrm{p}}^2 - \omega^2)l^2}$$

and $l = (2\varphi_0)^{-1/4}$ is the Thomas – Fermi screening length.

Matching together the electric potentials at $r = R$ gives us the equation

$$A\left(\frac{\sin kR}{kR^2} - \frac{\cos kR}{R}\right) = F\left[-R + \frac{\alpha(\omega)}{R^2}\right]. \tag{28}$$

Next we match the normal components of the vector of electric displacement:

$$A\varepsilon\,\frac{\mathrm{d}}{\mathrm{d}r}\left(\frac{\sin kr}{kr^2} - \frac{\cos kr}{r}\right)_{r=R} = -F\left(1 + \frac{2\alpha(\omega)}{R^3}\right). \tag{29}$$

Dividing (28) by (29) term by term, we eliminate F and A and find the dynamic polarizability

$$\alpha(\omega) = R^3\left[1 + \frac{3(1 - kR\cot kR)}{2(\varepsilon - 1)(1 - kR\cot kR) - \varepsilon(kR)^2}\right]. \tag{30}$$

As ought to be expected, the dynamic polarizability goes to infinity at eigen-frequencies given by Eqn (24). Equation (30) is an extension of Eqn (25) from Ref. [21] with due account for Thomas – Fermi screening.

Let us consider some extreme cases of the general expression (30). First we take the limit of very small clusters $R \ll l$ (no Thomas–Fermi screening). In the high-frequency limit $\omega \gg \omega_p$ from Eqn (30) we find

$$\alpha(\omega) = R^3 \left[\frac{4R^2}{15\pi l^2} - \frac{1}{3} \left(\frac{\omega_p}{\omega} \right)^2 \right] . \tag{31}$$

If $R/l \ll \omega_p/\omega \ll 1$, then from Eqn (31) it follows that

$$\alpha(\omega) = -\frac{n}{\omega^2} . \tag{32}$$

This agrees with the well-known high-frequency limit of dynamic polarizability [26] for $n = (4\pi R^3/3)N_e$ free electrons of the cluster.

If $\omega_p/\omega \ll R/l \ll 1$, then Eqn (31) predicts that

$$\alpha(\omega) = \frac{4}{15\pi} R^3 \left(\frac{R}{l} \right)^2 \ll R^3 . \tag{33}$$

In the static limit $\omega \to 0$, $\varepsilon \to -\infty$, from Eqn (30) we get

$$\alpha(0) = R^3 .$$

This is the well-known classical expression for the static polarizability of a small metallic sphere. Of course, if we take into account the diffusive nature of the electron cloud, then the static polarizability will increase compared with this value.

Finally, according to Eqn (31), we have $\alpha = 0$ when the frequency equals

$$\omega = \omega_p \sqrt{\frac{5\pi}{4}} \frac{l}{R} \gg \omega_p . \tag{34}$$

Figure 2 shows the dynamic polarizability $\alpha(\omega)$ as a function of frequency at $R/l = 0.5$ (weak Thomas–Fermi screening). In this limit, the resonance frequency is equal to the Mie frequency $\omega_p/\sqrt{3}$, in accordance with the results of the preceding section.

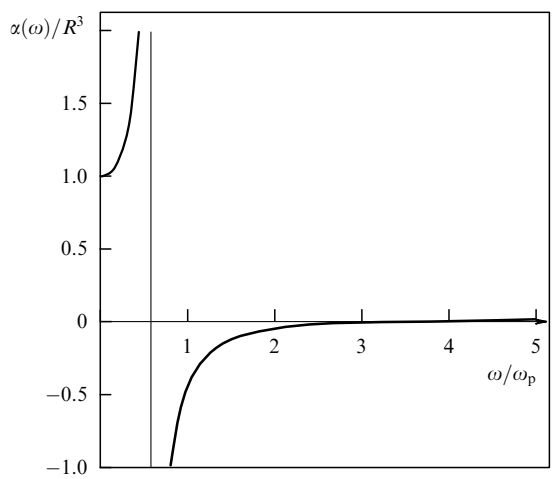

Figure 2. Dynamic polarizability of a small cluster ($R = 0.5l$) in units of the cube of the cluster radius vs. the ratio of the laser field frequency to the plasma frequency. Mie resonance is also shown.

Further we shall consider the limit of large clusters, $R/l \gg 1$, which corresponds to all real metallic clusters with the number of atoms $n \gg 1$. From Eqn (30) it follows that near the resonance frequency $\omega = \Omega$ [see Eqn (26)] the dynamic polarizability exhibits a resonance behavior

$$\alpha(\omega) = \frac{\text{const}}{\Omega^2 - \omega^2} . \tag{35}$$

The static polarizability in all cases is R^3.

The approximation of time-dependent local density, which is more complicated compared with the Thomas–Fermi approximation, was used for expressing the optical response in silver clusters [37]. The excitation energy of surface plasma oscillations was found to be about 4 eV, in agreement with the experimental data [38].

In Ref. [39], the imaginary part of the dynamic polarizability for a cluster containing about 100 atoms was calculated. The treatment was based anew on the time-dependent local density and the random phase approximation.

As the cluster expands after being acted on by a laser pulse, the frequency of surface plasma oscillations decreases with time. As shown in Ref. [20] in the framework of a random phase approximation, over 350 fs after the onset of expansion of a cluster comprizing 18 platinum atoms, this frequency decreases down to 1.5 eV, and as a result the resonance is attained with the frequency of the exciting laser pulse (Fig. 3).

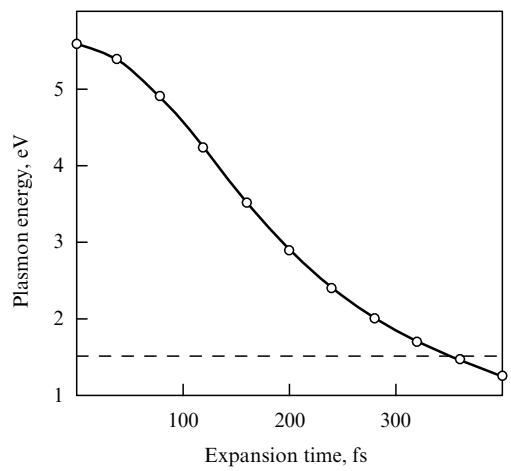

Figure 3. Plasmon energy vs. time for an expanding cluster consisting of 18 platinum atoms with the charge $Z' = 9$ [20]. The horizontal straight line indicates the energy of a photon of laser radiation.

Observe that the time-dependent Thomas–Fermi approximation can be derived from Vlasov equations by integrating the distribution function with respect to momenta [24]. As a result, the hydrodynamic equations of the electron concentration $N_e(r, t)$ and the local field of mean electron velocities $\mathbf{v} = \nabla\psi$ (where ψ is the velocity potential) are written in the form

$$\frac{\partial N_e}{\partial t} + \operatorname{div}(N_e \mathbf{v}) = 0 , \tag{36}$$

$$\frac{\partial \psi}{\partial t} + \frac{1}{2} (\nabla\psi)^2 + \frac{\delta H}{\delta N_e} = 0 . \tag{37}$$

Here H is the functional of total energy in the approximation of local density.

4.2 Hot cluster ions

Recently, the Thomas – Fermi model for an atom at arbitrary electron temperature was studied in detail by Pert [40]. Instead of using the stepwise distribution corresponding to zero temperature, the calculation of electron number density is based on the Fermi – Dirac distribution. In the general case, however, such calculations can only be numerical. Here we are going to consider the limit of high temperatures $T \gg E_{\mathrm{F}}$, which is realized when the clusters are exposed to the field of a superintense laser pulse (the values of the Fermi energy E_{F} are compiled in Table 1).

In the case of a hot cluster ion with $n \gg 1$ ions and $n - Z'$ electrons (where Z' is the charge of cluster), in accordance with the results of preceding section we start with the homogeneous bulk distribution of the charge in the cluster. Then the electric potential inside the ion sphere ($r < R$) can be found from the Gauss electrostatic law

$$\varphi(r) = \varphi(0) - \frac{2\pi}{3}\,\rho r^2 \,. \tag{38}$$

Here $\rho = Z'/(4\pi R^3/3)$ is the homogeneous charge density in the cluster ion. The potential (38) decreases on the cluster surface at $r \sim R$. Calculating the electron number density according to the classical Boltzmann equation (where T is the electron temperature)

$$N_{\mathrm{e}}(r) \sim \exp\left[\frac{\varphi(r)}{T}\right],$$

we find that a redistribution of electrons occurs: their concentration decreases at the cluster surface and accordingly increases in the bulk. Consequently, the density of the combined charge ρ of electrons and ions decreases inside the cluster and increases at its surface. This equalizes the electrostatic potential. As a result, one may suggest that the potential is a very smooth function of the radial coordinate r with the exception of a narrow region near the cluster boundary, where the potential falls off rapidly. The self-consistent electron distribution is given by the Poisson equation. Let us calculate this distribution under the assumption that $Z' \ll n$, i.e. the degree of ionization of the cluster is low.

For $r < R$, the Poisson equation reads as

$$\frac{\mathrm{d}^2\varphi}{\mathrm{d}r^2} + \frac{2}{r}\frac{\mathrm{d}\varphi}{\mathrm{d}r} = \frac{3}{r_{\mathrm{W}}^3}\left[\exp\left(\frac{\varphi - \varphi_0}{T}\right) - 1\right]. \tag{39}$$

Here, the constant quantity φ_0 is the analog of the chemical potential. We express the boundary conditions in the form

$$\frac{\mathrm{d}\varphi}{\mathrm{d}r}(r=0) = 0\,, \qquad \varphi(R) = \frac{Z'}{R}\,, \qquad \frac{\mathrm{d}\varphi}{\mathrm{d}r}(r=R) = -\frac{Z'}{R^2}\,. \tag{40}$$

Assuming that the cluster is large, we disregard the difference between the radii of electron and ion spheres. For $r > R$, the solution is the Coulomb potential of the cluster ion with the charge Z':

$$\varphi(r) = \frac{Z'}{r}\,.$$

The number of electrons inside the cluster can be expressed in terms of the potential, thus giving

$$n - Z' = \frac{3}{r_{\mathrm{W}}^3}\int_0^R \exp\left(\frac{\varphi(r) - \varphi_0}{T}\right) r^2\,\mathrm{d}r\,. \tag{41}$$

This expression also follows from Eqn (39), if we multiply it by r^2 and integrate with respect to r with due account for the boundary conditions (40). By this means, condition (41) is not new, since it follows from equation (39) and boundary conditions (40).

To simplify our calculations, we introduce the notation

$$x \equiv \frac{r}{R}\,, \qquad \varphi(r) \equiv \frac{Z'}{R}\,\psi(r)\,.$$

Then equation (39) becomes (for $x < 1$)

$$\psi'' + \frac{2}{x}\,\psi' = \frac{3n}{Z'}\left\{\exp\left[\frac{Z'(\psi - \psi_0)}{RT}\right] - 1\right\}. \tag{42}$$

Here $\psi_0 \equiv (R/Z')\varphi_0$. The boundary conditions (40) are written in the form

$$\psi'(0) = 0\,, \qquad \psi(1) = 1\,, \qquad \psi'(1) = -1\,. \tag{43}$$

The solution for $x > 1$ is given by

$$\psi(x) = \frac{1}{x}\,. \tag{44}$$

Obviously, we have $\psi(x) \sim 1$ everywhere over the region of x variation.

Now we consider the boundary layer near the cluster surface, $x = 1$. The right-hand side of Eqn (42) can be expanded in a Taylor series, because in the neighborhood of $x = 1$ one finds

$$\frac{Z'}{RT}\left[\psi(x) - \psi_0\right] \ll 1\,.$$

Then we get a simple linear differential equation

$$\psi'' + \frac{2}{x}\,\psi' = \frac{3n}{RT}\left[\psi(x) - \psi_0\right].$$

We introduce a new function

$$\Phi(x) = \psi(x) - \psi_0$$

and substitute it into the previous equation:

$$\Phi'' + \frac{2}{x}\,\Phi' = \frac{3n}{TR}\,\Phi\,. \tag{45}$$

It should be recognized that the inequality $3n/RT \gg 1$ always holds for large clusters. We seek a solution of Eqn (45) in the form

$$\Phi(x) = B\,\frac{\sinh kx}{x}\,.$$

The factor k is given by

$$k = \sqrt{\frac{3n}{RT}}\,.$$

From boundary conditions (43) it follows that $\Phi'(1) = \psi'(1) = -1$. Therefore, we have for the constant

$$B = -\frac{2}{k}\exp(-k) \ll 1$$

and the function Φ is small compared to unity. Hence, one obtains

$$\psi(x) = \psi_0 - \frac{2}{k}\exp(-k)\,\frac{\sinh kx}{x}\,.$$

Since $\psi(1) = 1$, from the previous equation it follows that

$$\psi_0 = 1 + \frac{1}{k}\,.$$

We write out the final solution as

$$\psi(x) = 1 + \frac{1}{k}\left[1 - 2\exp(-k)\,\frac{\sinh kx}{x}\right].$$

This solution satisfies all three boundary conditions in Eqn (43). The electric potential that complies with all the boundary conditions for $r < R$ takes on the form

$$\varphi(r) = \frac{Z'}{R}\left\{1 + \frac{1}{k}\left[1 - 2R\exp(-k)\,\frac{\sinh(kr/R)}{r}\right]\right\}. \quad (46)$$

One may conclude that the electron distribution inside the cluster is quasi-homogeneous with a high accuracy, and deviates from such only near the cluster surface.

Let us verify condition (41) for the total number of electrons. Substituting Eqn (46) into Eqn (41) and expanding the integrand in a Taylor series, with due account for the inequality $k \gg 1$ we get

$$n - Z' = \frac{3}{r_{\mathrm{W}}^3}\int_0^R\left(1 + \frac{\varphi(r) - \varphi_0}{T}\right)r^2\,\mathrm{d}r$$
$$= n - \frac{6Z'\exp(-k)}{kTr_{\mathrm{W}}^3}\int_0^R \sinh\left(\frac{kr}{R}\right)r\,\mathrm{d}r\,.$$

Taking the integral, we arrive at

$$n - Z' = n - \frac{3Z'n}{k^2RT} = n - Z'\,,$$

which ought to be expected.

The distribution of electron concentration inside the cluster is

$$N_{\mathrm{e}}(r) = \frac{3}{4\pi r_{\mathrm{W}}^3}\exp\left[\frac{\varphi(r) - \varphi_0}{T}\right]$$
$$\approx \frac{3n}{4\pi R^3}\left[1 - \frac{2Z'\exp(-k)}{kTr}\sinh\left(\frac{kr}{R}\right)\right].$$

The electron concentration at the cluster surface itself ($r = R$) assumes the form

$$N_{\mathrm{e}}(R) = \frac{3n}{4\pi R^3}\left(1 - \frac{Z'}{kTR}\right).$$

As this takes place, the quantity

$$\frac{Z'}{kTR} = \sqrt{\frac{Z'^2}{3nTR}} \ll 1\,.$$

For example, with $T = 1$ keV, $n = 10^5$, $Z' = 10^4$, and $R = 100$ Å we find that this quantity amounts to 0.22.

Earlier we assumed that the spherical shape of the cluster is not affected by the laser pulse. This is true, however, only in the case of large clusters. Small clusters built up of polarizable particles in the field of laser radiation may form other equilibrium configurations, whose shape will depend considerably on the frequency of radiation [41].

5. Ionization of clusters

5.1 Internal ionization

For analysis we take a large cluster comprizing 10^5 atoms. The kind of atoms incorporating into the clusters exposed to superintense laser radiation is not important. Take, for example, sodium atoms ($Z = 11$), and a linearly polarized laser radiation field with peak intensity $I = 10^{15}$ W cm^{-2}, radiation frequency $\omega = 1$ eV, and pulse length $\tau = 50$ fs. The radius of such a cluster is $R = 100$ Å.

At first the laser pulse induces dipole excitation, which causes the center of mass of the cloud of valence electrons to oscillate about the ion sphere. These oscillations are surface plasma Mie oscillations (see previous section). The period of such oscillations for the cluster of sodium atoms is 1.5 fs. Very soon, however, the collective oscillations are perturbed because of the ionization of cluster atoms. The decay of the surface plasmon is similar to Landau damping. For clusters of 50–1000 atoms, the time of such relaxation of plasmon is about 10 fs. As the number of atoms n in the cluster further increases, this time decreases as $n^{-1/3}$.

The collisions of electrons with one another occur so often that there are no temperature gradients or other gradients in the cluster. The electron temperature in the cluster during the laser pulse may be as high as 1 keV (see the next section). The temperature field is uniform because of a good heat conduction. The energy distribution of electrons is isotropic and is described by the classical Maxwellian distribution. The regions where the Maxwellian distribution holds are schematically indicated in Fig. 4. Here, $v_T = \sqrt{T}$ is the thermal velocity of electrons, and $v_F = F/\omega$ is the field velocity. The

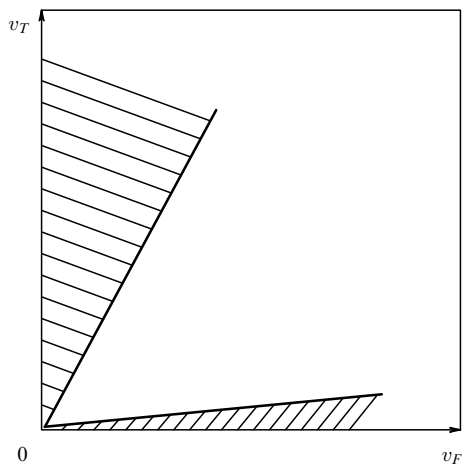

Figure 4. Ranges of applicability (hatched) of the Maxwellian distribution for the case $Z = 11$ [42]. The abscissa axis shows the field velocity of electron oscillations in the laser field; the ordinate axis shows the thermal velocity of electrons.

Maxwellian distribution of electrons holds good for weak laser fields, $v_T > v_F\sqrt{Z}$, and for very strong laser fields, $v_F > Zv_T$ [42].

The heating of an electron subsystem occurs mainly due to elastic electron – ion collisions (inverse bremsstrahlung), and because of other processes as well (see the next section). We shall see that the atoms in a cluster are completely ionized because of inelastic electron – ion collisions. Then the concentration of electrons becomes $N_e = ZN$, whereas the atomic number density for liquid metallic sodium is $N = 2.44 \times 10^{22}$ cm^{-3} (see Table 1).

The plasma in the cluster very soon comes to thermal equilibrium, because the characteristic time between the electron – electron collisions is small compared with the length of the laser pulse. This time may be estimated as [43]

$$\tau_{ee} = \frac{3T^{3/2}}{4\sqrt{2\pi}\,N_e \ln \Lambda} \sim 1 \text{ fs}. \tag{47}$$

Here $\ln \Lambda \sim 10$ is the typical value of the Coulomb logarithm. Such collisions represent one of the damping mechanisms, which bring the electron subsystem to the state of thermal equilibrium.

In all the above estimates we assume that the cluster is a small plasma sphere. Such an assumption is reasonable as long as the cluster radius R is large compared with the Debye screening radius r_D. At $T = 1$ keV, for the cluster of sodium atoms the Debye length is about

$$r_D = \sqrt{\frac{T}{4\pi N_e}} = 4.5 \text{ Å}.$$

In this section we consider the so-called *internal ionization,* when the electrons leave their atoms but remain within the bulk of a cluster. Internal ionization in clusters is mainly caused by inelastic electron – ion collisions. The equilibrium concentration N_Z of different atomic ions with the charge Z is given by the statistical Saha equation (if the equilibrium only depends on collisions) [44]

$$\frac{N_Z N_e}{N_{Z-1}} = 2\left(\frac{T}{2\pi}\right)^{3/2} \exp\left(-\frac{E_{Z-1}}{T}\right). \tag{48}$$

Here, E_{Z-1} is the ionization potential of an atomic ion with the charge $Z - 1$.

The condition of complete removal of electrons from all atomic shells may be approximated by the expression $N_Z = N_{Z-1} = N/2$, where Z is now the charge of an atomic nucleus ($Z = 11$ for our case of sodium atoms). Then the hydrogen-like ionization potential $E_{Z-1} \approx Z^2/2$, and the condition of complete stripping of all electron shells becomes ($N_e = ZN$)

$$ZN = 2\left(\frac{T^*}{2\pi}\right)^{3/2} \exp\left(-\frac{Z^2}{2T^*}\right). \tag{49}$$

In our case of sodium atoms, from this equation we get $T^* = 0.34$ keV. Table 2 gives the values of temperature T^* required for complete internal ionization of atoms in different metallic clusters, calculated according to Eqn (49).

In addition to inelastic electron – ion collisions, the internal ionization may be also due to the above-barrier ionization of atomic ions in the field of laser radiation.

Rhodes and colleagues [11, 45] suggested another mechanism of internal ionization of clusters comprizing inert gas atoms by the field of a superintense laser pulse. The pulse produces multiple ionization of simultaneously one or several valence shells (or the entire electron cloud of the atom depending on the pulse intensity). This takes place near the cluster surface, where the laser field is not shielded. The resulting n free electrons are regarded as *one quasi-particle* with the mass nm_e and charge ne, because it is compact enough compared with the distance to the nearest atoms in the sufficiently loose cluster of atoms of inert gas. This quasi-particle oscillates as a whole under the action of a laser field. In the course of such oscillations it collides with the adjacent atomic ions, and because of this the cross section of inelastic collisions is $n \gg 1$ times greater than that in the case of collisions of one electron. Further internal ionization of the cluster occurs through stripping of the internal atomic electrons by such a quasi-particle. This creates vacancies in the internal electron shells of atoms, and produces hard X-ray emission [12].

Ions with high multiplicity of charge (like Xe^{20+} or Kr^{18+}) are actually observed when clusters of inert gas atoms are exposed to superintense laser radiation (with intensity of order 10^{15} W cm^{-2}) [46]. This is not much different from the case of metallic clusters, since the initial ionization can be caused directly by the field of laser radiation. Figure 5 illustrates the production of multiply charged ions up to Xe^{20+}.

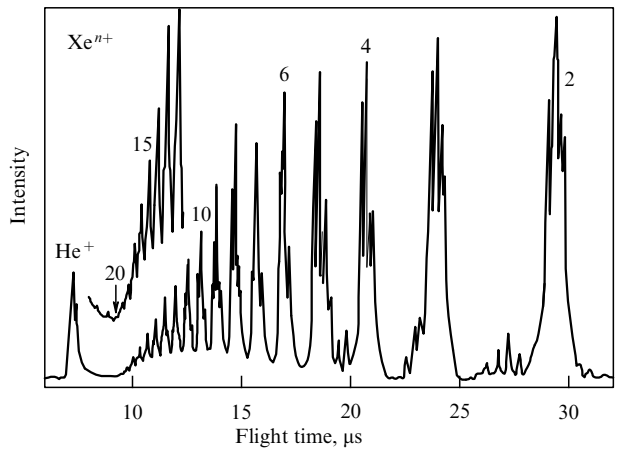

Figure 5. Time-of-flight spectrum of multiply charged cluster xenon ions produced by a laser with wavelength 624 nm [46].

5.2 Ionization by inelastic electron – ion collisions

Complete internal ionization of all atomic shells of the cluster discussed in the previous section takes a certain time, which

Table 2. Electron temperature T^* required for complete internal ionization of atoms in a cluster, and the exponent $u(T^*) = Z^2/2T^*$.

Atom	Li	Na	Al	K	Cu	Mo	Ag	Cs	W	Au
T^*, keV	0.046	0.34	0.50	0.78	2.06	3.77	4.54	4.90	10.2	11.4
$u(T^*)$	2.66	4.84	4.60	6.30	5.55	6.36	6.62	8.40	7.30	7.45

must be less than the length of the ultrashort laser pulse. Let us get some estimates for this time.

Multiple internal ionization is caused by inelastic collisions of hot electrons with multiply charged cluster ions. The cross section of this process (in atomic units) is given by the well-known semiempirical Lotz formula [47]

$$\sigma = 2.17q\,\frac{\ln(E/E_Z)}{EE_Z}\,. \tag{50}$$

Here, E is the kinetic energy of the striking electron, E_Z is the ionization potential of the atomic ion with charge Z, and q is the number of electrons in the atomic shell being ionized. Further we shall use the hydrogen-like value $E_Z = Z^2/2$. Therefore, the rate of the process in question is expressed from Eqn (50) as

$$w = N_{\rm e} v\sigma = \frac{17.34N}{vZ}\ln\frac{v}{Z}\,. \tag{51}$$

Here, v is the velocity of the striking electron, $N_{\rm e}$ is the electron concentration, and N is the number density of atoms in a cluster (all measured in atomic units).

The velocity of the electron has two components: the thermal velocity $\sqrt{T}$, and the induced field velocity F/ω. Typically, $\sqrt{T} > F/\omega$ (see estimates at the end of Section 2) and Eqn (51) ought to be averaged over a Maxwellian distribution. Assuming that $T \ll Z^2/2$ (see Table 2), we find

$$w = 13.8\,\frac{N\sqrt{T}}{Z}\exp\left(-\frac{Z^2}{2T}\right). \tag{52}$$

In the opposite limit of $\sqrt{T} < F/\omega$, we may simply substitute the value of $v = F/\omega$ into Eqn (51):

$$w = \frac{17.34\omega N}{FZ}\ln\frac{F}{\omega Z}\,. \tag{53}$$

Naturally, we assumed above that the impact ionization takes place at the maximum of the electric field strength $F\cos\omega t$. From Eqn (53) it is seen that this regime requires that the field strength should be limited from below: $F/\omega > Z$. This condition is stronger than the above condition $F/\omega > \sqrt{T}$.

In our example of cluster of sodium atoms at $T = 1$ keV, the intensity of laser radiation $I = 10^{15}$ W cm^{-2} (or field strength $F = 0.166$ a.u.), and the frequency of laser radiation $\omega = 1$ eV, we find that the ratio $\omega\sqrt{T}/F = 1.35$. Since $F/\omega = 4.5 < Z = 11$, the mechanism of ionization is thermal, and is governed by Eqn (52). For complete ionization of all atomic electron shells in the cluster made of sodium atoms, from Eqn (52) we get $w = 0.22$ fs^{-1}. This implies that electron–ion collisions occur very often during the ultrashort laser pulse.

5.3 Penetration of laser radiation into the cluster

The electromagnetic field of laser radiation penetrates into the cluster and decays there. The depth of penetration δ, associated with the excitation of plasma oscillations, may be identified with the imaginary part of the wavelength inside the cluster [48]:

$$\delta = \frac{c}{\omega\sqrt{|\varepsilon|}}\,. \tag{54}$$

The permittivity in this expression is given by

$$\varepsilon = 1 - \frac{4\pi ZN}{\omega^2} < 0\,. \tag{55}$$

In our case of a cluster of sodium atoms, for the visible spectral range we have $|\varepsilon| = 370$ and $\delta = 100$ Å. Accordingly, this component of the damping of laser radiation is not important. We may conclude that plasma oscillations can only be excited under resonance conditions.

The other component of damping is due to the electron–ion collisions. In the τ-approximation, the steady-state Boltzmann kinetic equation is written as (for $\omega \ll \nu_{\rm ei}$)

$$F\cos\omega t\,\frac{{\rm d}f_0}{{\rm d}v_x} = -\nu_{\rm ei} f'\,. \tag{56}$$

Here, f' is the small perturbation of the equilibrium Maxwellian distribution function f_0; x is the direction of the electric vector of linearly polarized laser radiation, and $\nu_{\rm ei}$ is the rate of elastic electron–ion collisions per unit time. The latter has a well-known form [43] [see also Eqn (47) above]

$$\nu_{\rm ei} = \frac{4\sqrt{2\pi}\,Z^2N}{3T^{3/2}}\ln\Lambda = 2.5\ {\rm fs}^{-1}\,. \tag{57}$$

We see that this quantity is on the order of the laser radiation frequency $\omega \approx 2$ fs^{-1}.

It should be emphasized that Eqn (57) holds good in the case of fast electrons ($T \gg Z^2$). In the event of slow electrons ($T \ll Z^2$), the situation is more complicated [49]. Expression (57) only holds when the laser radiation frequency complies with the condition $Z\omega \ll T^{3/2}$, when the electrons are mainly scattered through small angles. In the opposite case of $Z\omega \gg T^{3/2}$, the rate of electron–ion collisions depends on the laser frequency and may be written as [49]:

$$\nu_{\rm ei} = \frac{4\pi^{3/2}N}{15\times 3^{5/6}\sqrt{2T}}\,\frac{\Gamma(1/3)}{\Gamma(2/3)}\left(\frac{2Z^2}{\omega}\right)^{2/3}.$$

In this limit the scattering of electrons through large angles is important, and therefore the Coulomb logarithm is absent.

Let us calculate the mean energy received by the electron per unit time from a laser radiation field (recall the condition $\omega \ll \nu_{\rm ei}$):

$$\frac{{\rm d}E}{{\rm d}t} = \langle v_x F\cos\omega t\rangle = \frac{F^2}{2}\left\langle\frac{v_x}{\nu_{\rm ei}}\,\frac{{\rm d}f_0}{{\rm d}v_x}\right\rangle. \tag{58}$$

Here we have made the replacement $\langle\cos^2\omega t\rangle \to 1/2$. Taking in Eqn (58) the simple integral with the Maxwellian distribution function f_0 and considering Eqn (57), we find the specific power $P_{\rm a} = N_{\rm e}\,{\rm d}E/{\rm d}t$ absorbed per unit volume of the cluster:

$$P_{\rm a} = \frac{F^2}{Z\ln\Lambda}\left(\frac{2T}{\pi}\right)^{3/2}. \tag{59}$$

The intensity of laser radiation $I = cF^2/8\pi$ decreases with the field penetration depth z into the cluster. The corresponding equation is written as

$$\frac{{\rm d}I}{{\rm d}z} = -P_{\rm a} = -\frac{8\pi}{cZ\ln\Lambda}\left(\frac{2T}{\pi}\right)^{3/2} I\,. \tag{60}$$

Its solution corresponds to exponential damping of radiation:

$$I(z) = I_0 \exp\left(-\frac{z}{l}\right),$$

where the penetration depth l of laser radiation into the cluster is given by

$$l = \frac{cZ \ln \Lambda}{8\pi} \left(\frac{\pi}{2T}\right)^{3/2}. \tag{61}$$

In the event of a cluster of sodium atoms and the temperature $T = 1$ keV, we have $l = 1.7$ Å. This depth is small compared with the cluster radius R.

In the opposite limit $\omega \gg \nu_{\rm ei}$, the specific power absorbed by unit volume of the cluster is given by the known relationship in the theory of induced bremsstrahlung at electron – ion collisions [50]:

$$P_{\rm a} = \frac{F^2}{\omega^2} \nu_{\rm ei} N_{\rm e} = I \frac{32\pi\sqrt{2\pi}\, Z^3 N^2}{3c\omega^2 T^{3/2}} \ln \Lambda. \tag{62}$$

Observe that the quantity F^2/ω^2 is defined as the energy acquired by the electron from electromagnetic field at each collision with the ion. In this limit, the depth of laser radiation penetration into the cluster is

$$l' = \frac{3c\omega^2 T^{3/2}}{32\pi\sqrt{2\pi}\, Z^3 N^2 \ln \Lambda} = 1.5 \text{ Å}. \tag{63}$$

We see that in both limits, $\omega \ll \nu_{\rm ei}$ and $\omega \gg \nu_{\rm ei}$, the depth of penetration of laser radiation into the cluster is small compared to its radius. The above results hold for homogeneous plasmas.

Multiple internal ionization can also be caused by free electrons near the cluster surface: these electrons receive from the electromagnetic field an energy on the order of the ponderomotive energy $F^2/4\omega^2$. Such a mechanism is efficient in the case of long-wave laser radiation [51].

Therefore, we may conclude that the laser radiation does not go deep inside the cluster, and is absorbed in a thin layer near the surface (of course, most of the laser radiation is reflected from the cluster). Absorption is caused by the effective electron – ion collisions.

5.4 External ionization

Consider ionization of the entire cluster — that is, removal of electrons from the cluster to infinity with the formation of a cluster ion. In the case of a metallic cluster initially there are the conduction electrons of the cluster. The first mechanism of ionization consists in the removal of these electrons from the surface of the cluster by an external electromagnetic field (*cold* ionization). This process ends when the force of electron attraction to the resulting cluster ion exceeds the force acting from the side of the electromagnetic field. The charge of cluster ion Z' corresponding to the end of this process can be found from the Coulomb law:

$$Z' = FR^2. \tag{64}$$

For example, for an intensity of laser radiation $I = 10^{15}$ W cm^{-2} (field strength $F = 8.5 \times 10^8$ V cm^{-1}) and $R = 215$ Å, we find $Z' = 27{,}200$. The number of electrons released by this mechanism is small compared with the total number of electrons in the hot cluster of sodium atoms (the latter is $Zn = 1.1 \times 10^7$).

The authors of Ref. [52] studied the initial multiple ionization of large clusters made up of noble gas atoms through suppression of the electrostatic potential barrier by a superstrong electromagnetic field. It is assumed that such electrons leave both the parent atom and the cluster within characteristic atomic time. In the framework of the one-dimensional model, the example of ionization of a cluster consisting of 1100 xenon atoms in a laser field of intensity 10^{16} W cm^{-2} was considered. It was found that the above-barrier ionization results in the formation of a cluster ion with the charge $Z' = 1200$. Further ionization follows an alternative mechanism. The equilibrium state of the resulting cluster ion may be regarded as a conducting sphere with the charge concentrated in a thin surface layer (see Section 4). The superstrong Coulomb field in this layer knocks out additional electrons from atomic ions in the direction of the cluster center. These electrons accelerate to a high velocity and then leave the cluster. As a result, the charge of the cluster ion increases to $Z' = 2600$. This is the so-called *ignition mechanism* [53]. For example, the electric field strength at the surface of a cluster comprizing 25 neon atoms, when all atoms are singly ionized, is on the order of $F = 5 \times 10^{12}$ V cm^{-1}. The above-barrier ionization in such a field is very strong, and in turn leads to a further increase of the field strength (hence the name of the mechanism). Thus the fields created at the early stage of ionization 'ignite' the cluster and cause further ionization.

In the case of clusters of noble gas atoms the situation is rather similar to that with the metallic clusters. Of course, in the cluster made up of atoms of noble gases there are no conduction electrons prior to exposure to laser radiation. However, the above-barrier ionization of noble gas atoms and atomic ions by the field of laser radiation quickly gives rise to conduction electrons. The Bethe condition for above-barrier ionization has a simple form [54, 55]

$$F \geqslant \frac{E_Z^2}{4Z}, \tag{65}$$

where E_Z is the ionization potential of an atomic ion, and Z is the charge of this ion. For example, for neon atoms $E_1 = 21.5$ eV, and single ionization of all atoms in the cluster takes place when the field strength reaches $F = 8.0 \times 10^8$ V cm^{-1}. Such ionization occurs very fast (on the atomic time scale, i.e. about 0.01 fs). However, according to Eqn (65), the above-barrier ionization of the resulting atomic ion Ne^+ by such a field is not possible, because the ionization potential of this ion is 41.0 eV, which corresponds to a field strength $F = 1.5 \times 10^9$ V cm^{-1}. Of course, tunnel ionization is still possible, but it takes a very long time.

Using Eqns (64) and (65) we can find the degree of external ionization of the cluster Z', feasible through the 'ignition' mechanism. Eliminating the field strength F from these equations, one finds

$$Z' = \frac{R^2 E_Z^2}{4Z}.$$

For example, for a cluster of 1000 xenon atoms we get $R = 25$ Å, and for total double ionization of xenon atoms we have $Z' = 330$.

Experimental data for clusters of CH_2I molecules exposed to the radiation of a femtosecond titanium – sapphire laser

with the wavelength 795 nm [56] indicate that ionization of these clusters may be explained both by the ignition mechanism and by the model of coherent electron motion [11].

One further mechanism of electron emission from the cluster surface is a common thermal emission. It is described by the known Richardson – Dashman formula for the thermionic current from the spherical surface of the cluster (in atomic units) [57, 58]:

$$\frac{\mathrm{d}Z'}{\mathrm{d}t} = A_0 T^2 4\pi R^2 \exp\left(-\frac{J_{Z'}}{T}\right). \tag{66}$$

Here $A_0 = 1/(2\pi^2)$ is the so-called Richardson parameter. The quantity $J_{Z'} = Z'/R$ is defined as the ionization potential of a cluster ion with the charge $Z' \gg 1$, when the work function may be disregarded.

This result is confirmed by the experimental data [59] (Fig. 6). According to Eqn (66), the logarithm of the electron emission rate for small anion clusters of tungsten with a number of particles from 4 to 20 is a linear function of the inverse temperature $1/T$.

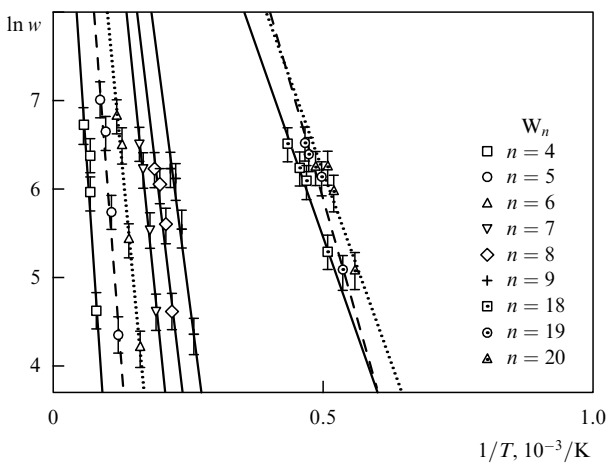

Figure 6. Experimental values of the probability of electron emission per unit time vs. inverse electron temperature for cluster tungsten anions with different numbers of particles n [59]. The rate of electron emission is measured in units of s^{-1}.

Integrating Eqn (66) over the time τ of action of the laser pulse, we obtain the final charge of the cluster ion (with due account for the inequality $J_{Z'} \gg T$):

$$Z' = TR \ln \frac{2TR\tau}{\pi} \gg TR. \tag{67}$$

For the above example of a cluster of sodium atoms, we have $Z' = 240{,}000$. It follows that thermal electron emission is a much more efficient mechanism of cluster ionization than the field (cold) emission. With a field intensity $I = 10^{15}$ W cm^{-2}, we find that from a sodium cluster of 10^6 atoms (containing a total of 1.1×10^7 electrons) about 270,000 electrons are emitted. The degree of ionization of the cluster is nonetheless low: for the tungsten cluster above it is as low as 2.4%. Similar simple calculations can be done on the basis of above relations for other metallic clusters and clusters of inert gas atoms with an arbitrary number of particles and other parameters.

The ionization of small clusters ($n < 100$) exposed to intense laser pulses was studied in Ref. [60] using the time-dependent density functional method based on the Boltzmann distribution. Notice that the Vlasov equations are a quasi-classical approximation to this method.

In the framework of the same method, it was demonstrated in Ref. [30] that most of the emitted electrons leave the cluster at the initial stage of the laser pulse, namely, 5 to 10 fs after the pulse is switched on.

According to the experimental findings of Ref. [18], increasing the duration of the laser pulse leads to a more efficient external ionization of metallic clusters. The additional ionization is due to the removal of electrons from atomic ions in the course of the Coulomb explosion of the cluster. A certain contribution may come from the tunnel ionization by long laser pulses. The calculation of its probability may be done with the Ammosov – Delone – Kraĭnov model [61].

The energy spectra of photoelectrons were calculated in Ref. [62] for the metallic clusters containing about 100 atoms. Similarly to the atomic case, the number of photoelectrons decreases exponentially as their kinetic energy increases.

Yet another mechanism of external ionization of clusters was proposed in Ref. [63]. Here, the intensive Mie resonance was studied for a spherical cluster ion of Na_{93}^{+}, excited by a femtosecond laser, which resulted in the external ionization of this cluster ion. The dimensions of cluster ions and their charge distributions were measured. The yield of a large number of doubly and triply charged cluster ions was observed. At the same time, this effect was absent when the cluster was exposed to a nanosecond laser pulse with the same wavelength and pulse energy. The process of efficient external ionization by a short laser pulse is attributed to autoionization associated with the excitation of the Mie resonance. A simple estimate of the lifetime of Mie resonance gives something like 10 fs.

We close this section with the following remarks:

(1) The ionization of large clusters exposed to intense ultrashort laser pulses occurs through thermal electron emission from the cluster surface;

(2) The degree of ionization is low;

(3) The laser radiation does not penetrate inside the cluster because of the strong absorption on the surface: the electrons absorb electromagnetic energy in the course of elastic collisions with ions.

6. Radiation absorption by a cluster

In this section we shall consider the process of absorption of electromagnetic radiation by a heated cluster. The observed absorption cross section may be approximated with the Lorentz curve [64, 65] (in some cases its shape will be more complicated [66, 67]):

$$\sigma_{\mathrm{a}}(\omega) = \sigma_{\max} \frac{\Gamma^2}{(\omega - \omega_0)^2 + \Gamma^2}.$$

Here, ω is the frequency of radiation, ω_0 is the resonance frequency, Γ is the width of the resonance curve, and $\sigma_{\max}$ is the maximum absorption cross section.

There are two mechanisms of radiation absorption. The first depends on the surface plasma oscillations, and $\omega_0 = \omega_{\mathrm{p}}/\sqrt{3}$ is the Mie frequency [5]. The second mechanism is associated with transitions between the states of individual

atomic ions in the cluster [68]. Then ω_0 is the frequency of such a transition. In both cases the absorption cross section is proportional to the number $n'(T)$ of conduction electrons in the cluster at the given (high) electron temperature. For example, for the cluster of potassium atoms we have

$$\sigma_{\max} = (3.4 \pm 0.6) \times 10^{-17} n' \text{ cm}^2 .$$

The number n' increases with a rise in temperature. Hereafter we shall not specify the mechanism of radiation absorption, assuming simply that its cross section does not depend on the intensity of laser radiation.

The energy balance equation for a heated cluster ion with charge Z' is written as

$$\frac{\mathrm{d}}{\mathrm{d}t}(Z' J_{Z'}) + \frac{3}{2}\frac{\mathrm{d}(n'T)}{\mathrm{d}t} = I\sigma_{\mathrm{a}}(n')n . \tag{68}$$

Here, n is the number of atoms in the cluster, I is the intensity of laser radiation, and $J_{Z'}$ is the ionization potential of a cluster ion (see Section 2).

The first term on the left-hand side of Eqn (68) corresponds to the energy of electrons leaving the cluster per unit time, while the second describes the heating of cluster electrons. The right-hand side of Eqn (68) is defined as the energy of laser radiation absorbed by the cluster per unit time. It is well to bear in mind that the exchange of energy between two electrons therewith occurs much more readily than the exchange of energy between the electron and ion. Because of this, the electrons obey the Maxwellian distribution, and it is possible to define the electron temperature T. The thermal energy of electrons is much higher than the Fermi energy (see Table 1). As a consequence, the thermal energy of electrons is the classical $3T/2$.

As indicated above, the evaporation of electrons is similar to the well-known thermionic emission [57, 58], while the field emission may be neglected. For the thermionic current one may use the well-known Richardson – Dashman formula (66). From Eqn (67) it follows that the following relationship holds with a logarithmic accuracy:

$$J_{Z'} = CT , \tag{69}$$

where $J_{Z'} = Z'/R$, and the quantity

$$C = \ln\left(\frac{2TR\tau}{\pi}\right) \tag{70}$$

with a logarithmic accuracy may be regarded as constant. Up to the logarithmic accuracy we also replaced the current time t by the duration of the laser pulse τ. We emphasize once again that the work function is neglected in the ionization potential. Finally, we find

$$Z' = CRT . \tag{71}$$

Thus, the energy balance equation (68) can be rewritten as

$$\frac{\mathrm{d}}{\mathrm{d}t}\left(\frac{3}{2}n'T + C^2RT^2\right) = I\sigma_{\mathrm{a}}(n')n = I\sigma_{\mathrm{a}}(n)n' .$$

Integrating this equation with respect to time, for the electron temperature T after cessation of a laser pulse we get

$$T\left(1 + \frac{2}{3n'}C^2RT\right) = \frac{2}{3}I\sigma_{\mathrm{a}}(n)\tau . \tag{72}$$

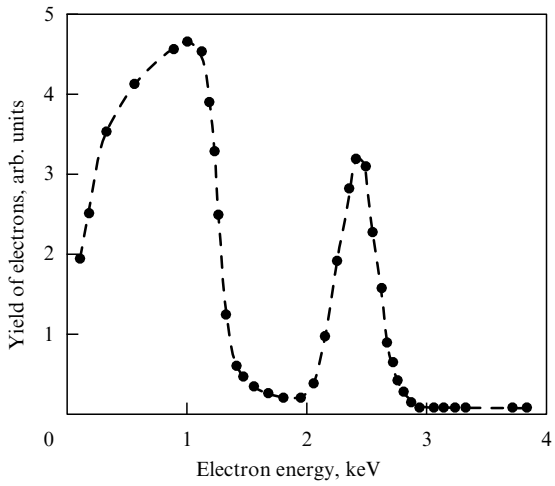

Figure 7. Experimental energy spectrum of electrons for the cluster of 2100 xenon atoms [6].

Consider an example of a cluster of $n = 10^5$ sodium atoms exposed to a laser pulse of length $\tau = 50$ fs and peak intensity $I = 10^{15}$ W cm^{-2}. In this case the absorption cross section is $\sigma_{\mathrm{a}}(n) \approx 0.7$ Å^2, and $R = 100$ Å. From Eqn (70) we find that the constant $C = 12$. Getting ahead we assume that the cluster is heated so strongly that each sodium atom loses all of its 11 electrons (see Table 2), and so $n' = 1.1 \times 10^6$. From Eqn (72) then it follows that after a laser pulse ceases the electron temperature is $T = 1$ keV. This estimate is confirmed by the experiment [6] (Fig. 7).

In Ref. [69], the electrons were observed with temperatures from 1 to 2 eV, emitted by clusters made up of $n = 1000 - 2000$ xenon atoms. These clusters were exposed to laser pulses with a peak intensity $I = 10^{16}$ W cm^{-2}.

Coulomb collisions of high-energy electrons with cold ions may be accompanied by the transfer of thermal energy from electrons to ions. The time of equalization of electron temperature T and ion temperature T_{i} is given by

$$\tau_{\mathrm{eq}} = \frac{3M_{\mathrm{i}}}{4\sqrt{2\pi}\,NZ^2 \ln\Lambda}\left(T + \frac{1}{M_{\mathrm{i}}}T_{\mathrm{i}}\right)^{3/2} .$$

Here M_{i} is the mass of an ion. From this expression it follows that, for example, for a cluster of argon atoms with $Z = 8$ and electron temperature $T = 1$ keV (the ions are assumed to be cold from the start), the time of equalization of the two temperatures is about 30 ps. Thus, this mechanism of energy transfer is entirely irrelevant to clusters heated by femtosecond laser pulses. The predominant mechanism of energy transfer from electrons to ions is associated with the radial expansion of the cluster (see Section 9).

7. X-ray emission

7.1 Statistical equilibrium with X-ray emission taken into account

Emission by multiply charged ions changes the statistical equilibrium between atomic ions with different charges Z. Let

us consider a simplified scheme of this emission process together with the collision excitation and ionization:

$$A^{+(Z-1)} + \mathrm{e} \to A^{+(Z-1)^*} + \mathrm{e}\,,$$
$$A^{+(Z-1)^*} + \mathrm{e} \to A^{+Z} + 2\mathrm{e}\,,$$
$$A^{+(Z-1)^*} \to A^{+(Z-1)} + \omega\,. \tag{73}$$

Here A^{+Z} characterizes the ground state of the atomic ion with a charge Z, and A^{+Z^*} the excited state of this ion. The decay of an excited state may take either of two channels: further ionization or emission of an X-ray photon and return to the ground state.

The probability of excitation [the first line in Eqn (73)] at electron–ion collision may be expressed from the known semiempirical relations [70]. In particular, the probability of excitation of multiply charged ions from the ground hydrogen-like state to the first excited state is (a.u.)

$$k_{\mathrm{exc}} = \frac{4.62}{Z^3}\,\frac{\sqrt{u(1+u/4)}}{1+3u/2}\,\exp\left(-\frac{3u}{4}\right)\ln\left(16+\frac{4}{3u}\right). \tag{74}$$

Here we used the notation

$$u \equiv \frac{Z^2}{2T}\,. \tag{75}$$

The rate constant for the backward process of excitation quenching can be found from Eqn (74) on the basis of the detailed balance principle, assuming that the concentrations of ions in the ground state and in the excited state obey the Boltzmann distribution law

$$k_{\mathrm{q}} = k_{\mathrm{exc}}\,\frac{g_0}{g_{\mathrm{exc}}}\,\exp\left(\frac{3u}{4}\right). \tag{76}$$

The ratio of statistical weights for the hydrogen-like 1s–2p transition is $g_{\mathrm{exc}}/g_0 = 3$. Substituting Eqn (74) into Eqn (76) we find

$$k_{\mathrm{q}} = \frac{1{,}54}{Z^3}\,\frac{\sqrt{u(1+u/4)}}{1+3u/2}\,\ln\left(16+\frac{4}{3u}\right). \tag{77}$$

Now we intend to analyze the process [second line in Eqn (73)]

$$A^{+(Z-1)^*} + \mathrm{e} \to A^{+Z} + 2\mathrm{e}\,,$$

taking into account only the first excited 2p state considered above. The Saha equation of statistical equilibrium for this process is given by

$$\frac{N_Z N_{\mathrm{e}}}{N^*_{Z-1}} = \frac{2}{3}\left(\frac{T}{2\pi}\right)^{3/2}\exp\left(-\frac{J^*_{Z-1}}{T}\right). \tag{78}$$

In this equation, the numeral 3 comes from the statistical weight of the 2p state, and the numeral 2 is that of the electron with two spin projections. The quantity N_Z is the concentration of atomic ions with charge Z in the ground 1s state, N_{e} is the electron concentration, and N^*_{Z-1} is the concentration of ions with charge $Z-1$ in the excited 2p state. The ionization potential of these ions is approximately equal to $J^*_{Z-1} \approx Z^2/8$.

Finally, in the case of the process

$$A^{+(Z-1)^*} \to A^{+(Z-1)} + \omega$$

[third line in Eqn (73)], the linkage between the concentrations of these components at statistical equilibrium is again given by the Saha equation

$$\frac{N^*_{Z-1}N^{\mathrm{ph}}_{\mathrm{e}}}{N_{Z-1}N^{\mathrm{ph}}_{\mathrm{a}}} = 3\exp\left(-\frac{J_{Z-1}-J^*_{Z-1}}{T}\right). \tag{79}$$

Here, $J_{Z-1} \approx Z^2/2$ is the ionization potential for the ground 1s state, the quantity

$$N^{\mathrm{ph}}_{\mathrm{a}} = N_{\mathrm{e}} k_{\mathrm{q}} \tau_{\mathrm{r}}$$

is the number of photons absorbed in the 1s state of the atomic ion, and τ_{r} is the radiative lifetime for the spontaneous 2p–1s transition. Finally, the quantity

$$N^{\mathrm{ph}}_{\mathrm{e}} = N_{\mathrm{e}} k_{\mathrm{q}} \tau_{\mathrm{r}} + 1$$

is defined as the number of photons emitted from the 2p state (according to the Einstein relation). In the hydrogen-like approximation, the spontaneous emission lifetime is given by

$$\tau_{\mathrm{r}} = \frac{\tau_0}{Z^4}\,, \qquad \tau_0 = 1.6\ \mathrm{ns}\,.$$

In all the cases considered here the following inequality $N^{\mathrm{ph}}_{\mathrm{a}} \ll 1$ is satisfied.

Multiplying equations (78) and (79) term by term, we find

$$\frac{N_Z N_{\mathrm{e}}}{N_{Z-1}}\left(1+\frac{1}{N_{\mathrm{e}} k_{\mathrm{q}} \tau_{\mathrm{r}}}\right) = 2\left(\frac{T}{2\pi}\right)^{3/2}\exp\left(-\frac{J_{Z-1}}{T}\right).$$

The condition of total ionization of all atomic shells of atomic ions in the cluster, with due account for the resonant-excited state, is written as $N_Z = N_{Z-1}$, where Z is now the charge of an atomic nucleus. This gives us the equation for the temperature T_{b} required for achieving the total ionization:

$$1+\frac{1}{N_{\mathrm{e}} k_{\mathrm{q}} \tau_{\mathrm{r}}} = \frac{2}{N_{\mathrm{e}}}\left(\frac{T_{\mathrm{b}}}{2\pi}\right)^{3/2}\exp\left(-\frac{J_{Z-1}}{T_{\mathrm{b}}}\right). \tag{80}$$

For example, in the event of a cluster of molybdenum atoms, we find $T_{\mathrm{b}} = 28$ keV. This magnitude is much greater than T^* (see Table 2). The same applies to clusters of other atoms. This allows us to conclude that in the case under consideration the collisional excitation is not efficient, and it is the direct ionization that works.

7.2 Reabsorption of resonant photons

Let us consider the reabsorption of resonant photons in cluster plasmas. Owing to reabsorption, the effective lifetime of resonance-excited states of atomic ions is increased. We shall calculate the line broadening caused by the resonance radiative transitions according to Holtzmark. Such broadening is produced by the static Coulomb fields of the surrounding atomic nuclei with charge Z. Then for the absorption cross section we find

$$\sigma_{\mathrm{a}} = \left(\frac{\pi c}{\omega}\right)^2 \frac{g_{\mathrm{exc}}}{g_0}\,\frac{1}{\tau_{\mathrm{r}}\Delta\omega}\,.$$

Here the spectral linewidth according to Holtzmark is [70]

$$\Delta\omega = 12.5(n'^2 - n^2)N^{2/3} = 37.5N^{2/3}\,.$$

The frequency of the 2p – 1s transition is $\omega = 3Z^2/8$; $n = 1$ and $n' = 2$ are the principal quantum numbers of the states participating in the radiative transition.

Thus, the absorption cross section for such a transition may be represented as

$$\sigma_{\rm a} = \left(\frac{8\pi c}{3}\right)^2 \frac{1}{12.5\tau_0 N^{2/3}}$$

(the charge Z of the nucleus is eliminated from this expression). As before, $\tau_0 = 1.6 \times 10^{-9}$ s. This expression for the absorption cross section may be used in calculating the universal probability of reabsorption of a resonant photon in the center of the spectral line on a spherical cluster of radius R:

$$\eta = \sigma_{\rm a} RN = \sigma_{\rm a} r_{\rm W} n^{1/3} N = \left(\frac{8\pi c}{3}\right)^2 \frac{r_{\rm W} N^{1/3}}{12.5\tau_0}\, n^{1/3} = 10^{-3} n^{1/3}\,.$$

Here, $r_{\rm W}$ is the Wigner – Seitz radius (see Table 1), and n, as before, is the number of atoms in the cluster. The quantity N does not enter this expression. We see that even for clusters with $n = 10^6$ we have $\eta = 0.1$. In this way, reabsorption of resonant photons is not an important process for the cluster plasmas in question.

The effective excitation of the upper level in the atomic ion with X-ray emission taken into account was considered in Ref. [71]. It was shown that the reinforcement of X-ray emission may be accomplished as a result of Coulomb explosion of the cluster.

7.3 Emission of resonant photons

From Eqn (79) it follows that the equilibrium number of atomic ions excited to a resonance state is

$$N^*_{Z-1} = \frac{N_{\rm a}^{\rm ph}}{N_{\rm e}^{\rm ph}}\, 3N_{Z-1} \exp\left(-\frac{3u}{4}\right). \qquad (81)$$

Here (as before) we used the notation $u = Z^2/2T$. The power of resonant photon emission in a cluster plasma takes the form

$$P_{\rm r} = \frac{N^*_{Z-1} N_{\rm e}^{\rm ph} \hbar\omega}{\tau_{\rm r}}\,,$$

where $\hbar\omega = 3Z^2/8$ is the energy of a photon emitted in the 2p – 1s transition. This power is reduced to the unit volume of cluster plasma. Substituting Eqn (81) into this expression, we get

$$P_{\rm r} = \frac{9}{16} Z^3 N^2 k_{\rm q} \exp\left(-\frac{3u}{4}\right). \qquad (82)$$

As before, we assume that the ionization of atomic ions in the cluster is complete — that is, $N_{\rm e} = ZN$, $N_{Z-1} = N/2$.

Substituting Eqn (77) into Eqn (82), we represent the emitted power as

$$P_{\rm r} = 0.867N^2 \frac{\sqrt{u(1+u/4)}}{1+3u/2} \exp\left(-\frac{3u}{4}\right) \ln\left(16 + \frac{4}{3u}\right). \qquad (83)$$

Now we can calculate the maximum emitted power as a function of the electron temperature T (that is, as a function of the variable u). Such a maximum is attained at $u = 0.24$. Finally, we find (in atomic units)

$$P_{\rm r}^{\max} = 0.81N^2\,.$$

Table 3 gives the values of the maximum emitted power and the corresponding electron temperature for different metallic clusters.

Table 3. Parameters of cluster plasma, corresponding to the maximum power of emission by resonance-excited hydrogen-like ions.

Metal	Li	Na	Al	K	Cu
T, keV	0.5	6.9	9.6	20.5	47.7
$P_{\rm r}^{\max}$, 10^{19} W cm^{-3}	4.8	1.23	6.0	0.33	12.0

We see that the emitted specific power is sufficiently large. According to the results of the preceding section, the reabsorption of these resonant photons inside the cluster is not efficient, and so the photons are emitted outside the cluster.

7.4 Experimental results

The experiments proving the role of clusters in the emission of X-rays (with the photon energy of a few keV) were done with clusters of krypton atoms [72]. Transitions originating in the L shell were observed (wavelengths about 5 to 7.5 Å). The generation of instantaneous X-rays during the action of the laser pulse is attributed to the formation of vacancies in the inner shells of cluster atoms.

The results of measurements of the absolute yield of X-ray emission produced when the clusters of xenon atoms are exposed to 2-ps laser pulses are described in Ref. [73]. It was found that a laser pulse energy of 300 mJ corresponded to about 10-μJ energy of X-ray emission (per pulse) with a frequency above 1 keV. Some correlation between the yield of X-ray emission and the size of clusters was also observed.

Finally, the X-rays generated when large clusters of krypton atoms were exposed to high-intensity ultrashort laser pulses with an intensity above 5×10^{17} W cm^{-2} were studied in Ref. [17]. It was found that the X-ray emission is isotropic, and the highest conversion factor of the energy of IR laser radiation into X-ray emission amounts to 1.7×10^{-8}. The generation of X-rays was attributed to the appearance of strongly stripped atomic ions resulting from impact ionization of the atomic L shells by electrons in the laser-heated cluster plasma. Figure 8 shows the measured yield of X-ray emission as a function of the peak intensity I of laser radiation. We see that the signal of X-ray emission grows as $I^{3/2}$. Such behavior is explained simply by the increase of the focal volume with increasing intensity I, as soon as the yield of ions with a given multiplicity comes to saturation.

Strong X-ray emission was also found in Ref. [74], where large clusters with a radius of about 100 Å were exposed to high-power laser pulses. In this work it was found that resonant absorption is important in the process of the cluster interaction with the superintense laser radiation. For a given size of the cluster, there is an optimal length of the laser pulse that corresponds to the maximum absorption of laser radiation. The maximum absorption coefficient correlates with the maximum yield of soft X-ray emission. The authors

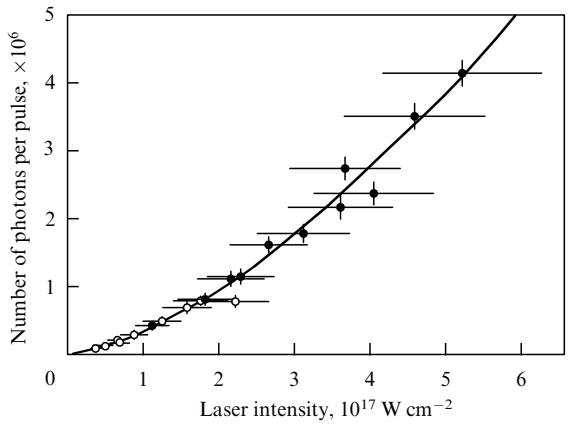

Figure 8. Measured yield of X-ray emission vs. peak intensity of a laser pulse [17]. X-rays are produced in radiative transitions to the L shell of atoms entering large krypton clusters.

of Ref. [74] were able to control the efficiency of conversion of laser radiation into X-ray emission by varying the length of the laser pulse.

X-ray emission by atomic clusters considerably depends on the wavelength of laser radiation. According to Ref. [75], the yield of X-ray emission (for the L shell, again) is approximately 3000 times greater when the clusters of xenon atoms are exposed to a UV pulse with wavelength 248 nm as compared with exposure to an IR pulse with wavelength 800 nm and the same intensity.

8. Generation of harmonics

A two-dimensional model for calculating the enhanced generation of harmonics by cluster argon ions exposed to an ultrashort (about 25 fs) laser pulse with moderate peak intensity (about 10^{14} W cm^{-2}) is presented in Ref. [76]. The intensity of lower harmonics (below the 15th) in the cluster was found to be about two orders of magnitude higher than that for atomic argon. Besides, the plateau in the curve of harmonic intensity vs. harmonic number is much longer for the argon cluster as opposed to the atomic argon. This is because the ionized clusters have not only a high ionization potential, but also a higher polarizability compared with the atomic ions.

A simple model of generation of harmonics in atomic clusters was proposed in Ref. [77]. The time-dependent Schrödinger equation was solved for a simplified one-dimensional system. The cluster was regarded as a one-dimensional chain of atoms aligned with the direction of polarization of laser radiation, whose intensity was varied in the range from 10^{13} to 10^{14} W cm^{-2}. The atoms in the chain were equidistant and were assumed to be one-electron atoms. The field of the atomic core was represented by a smoothed one-dimensional Coulomb potential. The main result of numerical calculations consists in that the clusters are a medium in which the generation of harmonics is much more efficient than in a medium of isolated atoms of the same kind. For not-too-high harmonics (9th – 13th) and for moderate laser intensities, the enhancement factor was about 10. Another general result is that the range of intensities corresponding to efficient generation of harmonics in clusters is much narrower than that for isolated atoms. However, when the intensity of laser radiation is high, the generation of harmonics in a medium of isolated atoms is comparable or even stronger than in a medium of clusters.

This is confirmed by the experimental results reported in Ref. [78]. It is demonstrated that a medium of intermediate-sized clusters of a few thousand atoms of inert gas is much better at generating the higher harmonics than a medium of isolated atoms of the same density. The enhancement factor for the 3rd – 9th harmonics is about 5. Also, the dependence of the efficiency of generation of harmonics on the intensity of laser radiation is much more articulate for clusters than for isolated atoms. The highest harmonic number for clusters is higher than that for the isolated atoms.

The authors of Ref. [79] provided arguments in favor of an N^3 law for the intensity of harmonics in clusters (N is the mean concentration of atoms), as opposed to the N^2 law for atomic gases.

Instead of generation of harmonics in small metallic clusters, the amplification of the incident femtosecond laser pulse was observed. Such amplification is due to the excitation of a surface plasma Mie resonance. Calculations based on the method of the density functional indicate that this effect does not depend on the size of the cluster. The same approach was used in Refs [80, 81] to show that the plasma Mie resonance is rather a sinusoidal oscillation, and so the generation of the higher harmonics of this resonance owing to anharmonicity of oscillations is not efficient.

9. Expansion of clusters

There are different mechanisms of expansion pertaining to clusters of noble gases when exposed to a laser pulse [3]. While an argon cluster may expand because of the Coulomb repulsion of its constituent atomic ions, the clusters of xenon atoms expand both because of the Coulomb repulsion of ions and the gas-dynamic expansion owing to the increased pressure inside the cluster. In particular, the kinetic energies of ions in the case of gas-dynamic expansion of large clusters of xenon atoms allow the assumption that the electron temperature is about 1.5 keV. However, the highest-energy ions are produced by electrostatic repulsion. The observed energy – charge dependences for the ions do not fit in with the conventional coronal plasma theory [82]. At the same time, the simple model of Coulomb explosion agrees well with the experiment [3].

The results of an experiment on the photoionization of clusters of inert gas atoms by a high-intensity femtosecond laser pulse (above 10^{16} W cm^{-2}) are presented in Ref. [6]. The energies of electrons and ions were measured after explosion of the cluster; they turned out to be fairly large. The energy distribution of electrons in the exploding cluster includes electrons with kinetic energies up to 3 keV, which is several orders of magnitude greater than the energies observed in the case of above-threshold ionization of individual atoms or molecules [61]. The average energies of ions produced in explosion of a cluster are tens of kiloelectron-volts, while the maximum energy of an ion was as large as 1 MeV (Fig. 9). Ions with charge numbers as high as Xe^{40+} were observed.

These experimental results are adequately explained by a theoretical model that regards the cluster as a small plasma ball. The cluster is ionized by the laser field and internal collisions (see above), and then starts to expand. As the cluster expands, the electron concentration decreases, and at some point in time the frequency of the laser field comes into resonance with the frequency of the surface Mie resonance.

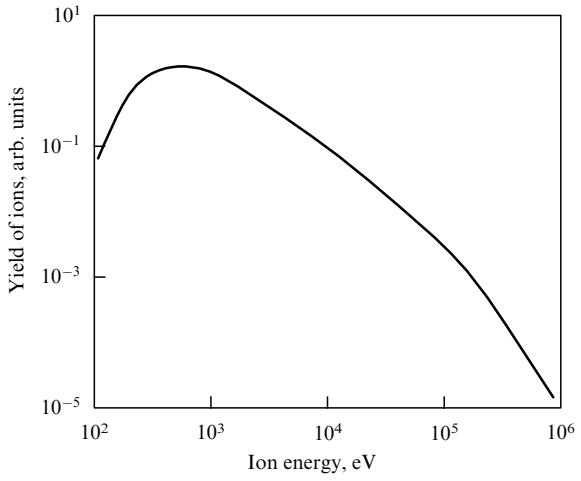

Figure 9. Experimental energy spectrum of ions for a cluster of 2500 xenon atoms [6] with a peak laser pulse intensity of 2×10^{16} W cm^{-2}.

This leads to a rapid transfer of electromagnetic energy to the electrons, causing a sharp peak in the electron temperature. At this instant the atomic ions of the cluster are vigorously stripped to high charge numbers by the hot electrons, and the cluster explodes. Such collective phenomena are very important in the case of a cluster, while being absent in the event of interaction of a laser field with individual atoms.

Explosions of clusters consisting of hundreds or thousands of atoms under the action of a superstrong laser pulse release ions with high energies and charges. The phenomenon is very similar to the expansion of solid-state laser-heated plasma into the vacuum. By contrast, the Coulomb explosions of small molecules and small clusters in strong laser fields only give rise to ions with small energies and charges.

In the framework of the classical two-fluid plasma model, one may ignore the inertia of electrons as compared with the inertia of the much more massive ions. Then the equations for the ionic liquid become [83]

$$\frac{\partial N_{\mathrm{i}}}{\partial t} + \operatorname{div}(N_{\mathrm{i}}\mathbf{v}_{\mathrm{i}}) = 0\,, \tag{84}$$

$$\frac{\partial \mathbf{v}_{\mathrm{i}}}{\partial t} + (\mathbf{v}_{\mathrm{i}}\nabla)\mathbf{v}_{\mathrm{i}} = -\frac{Z}{M_{\mathrm{i}}N_{\mathrm{i}}}\,\nabla p_{\mathrm{e}}\,. \tag{85}$$

Here, N_{i} is the concentration of atomic ions, $\mathbf{v}_{\mathrm{i}}$ is their velocity, M_{i} is the mass of an ion, Z is the charge of an ion, and p_{e} is the pressure of the electron subsystem. The first equation states the conservation of the number of ions, the second is defined as the momentum conservation law. The two equations describe the motion of an ionic liquid under the action of electron pressure. The high-temperature electrons produce the ambipolar potential that may accelerate the ions. The appropriate force stands on the right-hand side of Eqn (85).

To calculate this force, one needs to know the equation of state for the electrons. The simplest approximation takes advantage of the high heat conduction in cluster plasma and is expressed by the isothermal equation of state [6]. Notice that the actual expansion of a cluster is not isothermal: the electron temperature is a rather complicated function of time. From calculations made in Ref. [6] it follows that the explosion of a large cluster of xenon atoms is caused by the

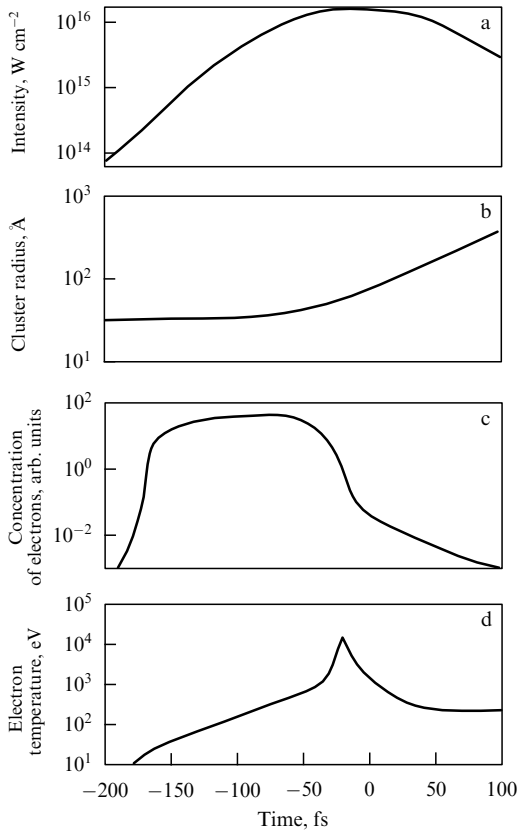

Figure 10. Theoretical evaluation of the evolution of cluster of 1800 xenon atoms (radius 30 Å) exposed to a laser pulse of length 140 fs and intensity 2×10^{16} W cm^{-2} [6]: (a) envelope of laser pulse; (b) radius of expanding cluster; (c) concentration of electrons, and (d) electron temperature.

gas-dynamic force represented by the right-hand side of Eqn (85) rather than by the Coulomb repulsion between the multiply charged atomic ions. A typical time history of the expanding cluster is shown in Fig. 10. The curve in Fig. 10d proves the above assumption of the high heat conductivity of cluster plasmas.

The measurement results on the kinetic energy of ions in large clusters of HI molecules (at room temperature) exposed to a strong femtosecond laser pulse are presented in Ref. [4]. Explosions of clusters give rise to protons with energies of a few keV, and iodine ions with energies of about 100 keV. It was demonstrated that clusters of heteronuclear diatomic molecules absorb the energy of laser radiation more efficiently than clusters of atoms or diatomic molecules containing two atoms of the same kind.

As indicated above, the laser field does not penetrate into the cluster, being absorbed on its surface. When the cluster explodes, however, its density is much reduced, and more of the laser radiation gets into the cluster. This leads to additional internal ionization in the expanding cluster [84]. For clusters of 1000 xenon atoms, the charge Z of xenon atomic ions produced in Coulomb explosion was from 8 to 18.

The stepwise explosion of atomic clusters in a strong laser field was considered in Ref. [85] in the context of the Thomas – Fermi model (detailed calculations for the one-dimensional case can be found in Ref. [86]). The explosion reveals the shell structure of the clusters, so the separate layers of the cluster explode in succession. The first ions have rather large kinetic energies because of Coulomb repulsion and the

efficient energy transfer from hot electrons to the outer layer of the cluster.

The multiply charged atomic ions produced by the Coulomb explosion lose the remaining electrons in the course of continued interaction with laser radiation, and their charge is increased. The results of experimental investigation of this process can be found in Ref. [87].

As shown in the recent experimental work [88], the explosion of clusters is enhanced when the clusters are exposed to two successive laser pulses of high intensity. In this work the energies of atomic ions resulting from the explosion of a cluster of xenon atoms were measured. The cluster was exposed to two femtosecond laser pulses: first at the frequency of the second harmonic (wavelength 390 nm), and then at the fundamental frequency (wavelength 780 nm). The intensity of each pulses was about 10^{15} W cm^{-2}. At some optimal lag between the two pulses the maximum energy of ions was increased twofold — from 100 to 200 keV. The laser pulse energy required to obtain a particular kinetic energy of the atomic ion turned out to be much smaller when the cluster was exposed to two pulses of different wavelengths as compared with the exposure to only one pulse. This effect is attributed to a much increased heating of cluster when the concentration of electrons (which decreases as the cluster expands) corresponds to the Mie resonance frequency for the field of the second harmonic: $\omega_{\mathrm{M}} = \sqrt{4\pi N_{\mathrm{e}}(t)/3} = 2\omega$. At some later point in time $t' > t$ the cluster is heated again when the Mie frequency occurs in resonance with the fundamental frequency of a laser: $\omega_{\mathrm{M}} = \sqrt{4\pi N_{\mathrm{e}}(t')/3} = \omega$. As a matter of fact, in the course of expansion of cluster we have $N_{\mathrm{e}}(t') < N_{\mathrm{e}}(t)$.

Figure 11 shows four snapshots of an argon cluster of 55 atoms at different instants of time in the course of exposure to a laser pulse with peak intensity 10^{15} W cm^{-2} [89]. Ions are represented by large circles, and the electrons by black dots. The cluster starts to expand 15 fs before the maximum intensity of the laser pulse is reached. By this time there are 427 free electrons resulting from the ionization of argon atoms (internal ionization). As follows from the figure, inside the cluster there are still about 100 electrons. The cluster itself expands isotropically. At the peak of laser intensity (at instant of time $t = 0$) there are still many electrons in the neighborhood of the expanding cluster. Twenty femtoseconds later the concentration of electrons in the cluster decreases, and the cluster proceeds to expand isotropically due to Coulomb repulsion of ions.

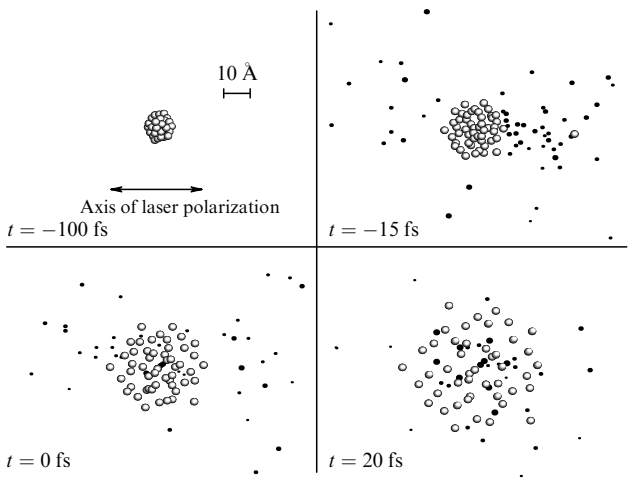

Figure 11. Snapshots of a cluster of 55 argon atoms at different times in the course of exposure to a 200-fs laser pulse [89]. The maximum of intensity corresponds to $t = 0$.

10. Conclusions

The recently published detailed review covers the properties of cluster plasma [25]. The present article deals with the evolution of large clusters exposed to superintense ultrashort laser pulses. The cluster is excited because of the interaction of the electron subsystem with the field of the laser pulse.

Both experimental and theoretical studies of the evolution of clusters exposed to superintense ultrashort laser pulses are currently still at their initial stage. Many issues discussed in this review call for further investigation, which may lead to revision of some of the results presented here. For example, the treatment of electron evaporation from the surface of a hot cluster is based on the well-known Richardson – Dashman formula which disregards the cluster charging in the course of evaporation. Such charging will certainly reduce the thermionic current from the cluster ion as its charge increases.

The role of the *surface* of cluster ion in the heating of electrons must also be studied in detail. The energy of a free electron in the cluster, which elastically bounces off the cluster surface back into the bulk in the presence of laser field, is augmented at each reflection by an increment of the order of the vibrational energy F^2/ω^2. Elastic reflection is due to the large charge of the cluster ion, caused by the strong external ionization. Today it is not clear how this effect competes with the induced inverse bremsstrahlung.

Recent studies of the photoionization of atomic clusters by high-intensity femtosecond laser pulses (10^{16} W cm^{-2} and higher) indicated that by exciting large clusters it is possible to obtain a superheated microplasma, which will emit atomic ions with a kinetic energy of up to 1 MeV. In particular, using deuterium clusters it is possible to produce plasma with a mean energy of ions sufficient for nuclear fusion. The observation of such a reaction in the explosion of deuterium clusters heated by a powerful laser with a high rate of pulse repetition was reported recently in Ref. [90]. As observed, the yield is about 10^5 neutrons per 1 J of incident energy of laser radiation (according to the nuclear reaction $\mathrm{d} + \mathrm{d} \rightarrow \mathrm{He}^3 + \mathrm{n}$). These results ought to stimulate further studies of thermonuclear fusion using small-size powerful lasers. A tabletop source of neutrons may have extensive applications in materials science.

This work was partly supported by the Russian Foundation for Basic Research (Grant #99-02-17810). One of the authors (M S) thanks the Max Born Institute in Berlin for support. Our thanks are due to W Becker for stimulating discussions of problems treated in this review.

References

1. Sullivan A et al. *Opt. Lett.* **21** 603 (1996)
2. Boehly T R et al. *Opt. Commun.* **133** 495 (1997)
3. Lezius M et al. *Phys. Rev. Lett.* **80** 261 (1998)
4. Tisch J W G et al. *Phys. Rev. A* **60** 3076 (1999)
5. Ditmire T et al. *Phys. Rev. A* **53** 3379 (1996)
6. Ditmire T et al. *Phys. Rev. A* **57** 369 (1998)
7. Hagena O F *Surf. Sci.* **106** 101 (1981)
8. Hagena O F *Rev. Sci. Instrum.* **63** 2374 (1992)
9. Wormer J et al. *J. Chem. Phys.* **75** 402 (1981)
10. Hagena O F, Obert W *J. Chem. Phys.* **56** 1793 (1972)

11. Boyer K et al. *J. Phys. B* **27** 4373 (1994)
12. Borisov A B et al. *J. Phys. B* **28** 2143 (1995)
13. Kondo K et al. *J. Phys. B* **30** 2702 (1997)
14. Schröder W A et al. *J. Phys. B* **31** 5031 (1998)
15. Honda H et al. *Phys. Rev. A* **61** 023201 (2000)
16. Lezius M et al. *J. Phys. B* **30** L251 (1997)
17. Dobosz S et al. *Phys. Rev. A* **56** R2526 (1997)
18. Döppner T et al. *Int. J. Mass Spectrom. Ion Processes* **192** 387 (1999)
19. Schumacher M et al. *Eur. Phys. J. D* **9** 411 (1999)
20. Köller L et al. *Phys. Rev. Lett.* **82** 3783 (1999)
21. Kresin V V *Phys. Rep.* **220** 1 (1992)
22. De Heer W A *Rev. Mod. Phys.* **65** 611 (1995)
23. Brack M *Rev. Mod. Phys.* **65** 677 (1995)
24. Calvayrac F et al. *Phys. Rep.* (2000) (in press)
25. Smirnov B M *Usp. Fiz. Nauk* **170** 495 (2000) [*Phys. Usp.* **43** 453 (2000)]
26. Kittel Ch *Introduction to Solid State Physics* 2nd ed. (New York: Wiley, 1971) [Translated into Russian (Moscow: Nauka, 1978)]
27. *Handbook of Chemistry and Physics* 79th ed. (Ed. D R Lide) (London: CRC Press, 1998 – 1999)
28. Gross E K U, Kohn W *Adv. Quantum Chem.* **21** 255 (1990)
29. Calvayrac F, Reinhard P G, Suraud E *Phys. Rev. B* **52** R17056 (1995)
30. Gross M, Guet C *Phys. Rev. A* **54** R2547 (1996)
31. Fomichev S V, Zaretsky D F *J. Phys. B* **32** 5083 (1999)
32. Ullrich C A, Reinhard P G, Suraud E *Phys. Rev. A* **57** 1938 (1998)
33. Smirnov M B, Kraĭnov V P *Zh. Eksp. Teor. Fiz.* **115** 2014 (1999) [*JETP* **88** 1102 (1999)]
34. Smirnov M B, Krainov V P *Laser Phys.* **9** 943 (1999)
35. Domps A, Reinhard P G, Suraud E *Eur. Phys. J. D* **2** 191 (1998)
36. Vinogradov A V, Shevel'ko V P *Tr. Fiz. Inst. Akad. Nauk SSSR* **119** 159 (1980)
37. Yabana K, Bertsch G F *Phys. Rev. A* **60** 3809 (1999)
38. Tiggesbäumker J et al. *Phys. Rev. A* **48** R1749 (1993)
39. Bertsch G F, Van Giai N, Vinh Mau N *Phys. Rev. A* **61** 033202 (2000)
40. Pert G J *J. Phys. B* **32** 249 (1999)
41. Claro F, Rojas R *Appl. Phys. Lett.* **65** 2743 (1994)
42. Chichkov B N, Shumsky S A, Uryupin S A *Phys. Rev. A* **45** 7475 (1992)
43. Silin V P *Zh. Eksp. Teor. Fiz.* **47** 2254 (1964) [*Sov. Phys. JETP* **20** 1510 (1965)]
44. Landau L D, Lifshitz E M *Statisticheskaya Fizika* 4th ed. (Statistical Physics) (Moscow: Nauka, 1995) Sect. 104 [Translated into English (Oxford: Pergamon Press, 1980)]
45. Boyer K, Rhodes C K *J. Phys. B* **27** L633 (1994)
46. Snyder E M, Buzza S A, Castleman A W *Phys. Rev. Lett.* **77** 3347 (1996)
47. Lotz W *Z. Phys.* **216** 241 (1968)
48. Landau L D, Lifshitz E M *Elektrodinamika Sploshnykh Sred* 2nd ed. (Electrodynamics of Continuous Media) (Moscow: Nauka, 1982) Sect. 93 [Translated into English (Oxford: Pergamon Press, 1984)]
49. Krainov V P *J. Phys. B* **33** 1585 (2000)
50. Fedorov M V *Elektron v Sil'nom Svetovom Pole* (Electron in Strong Light Field) (Moscow: Nauka, 1991)
51. LaGattuta K J *Eur. Phys. J. D* **2** 267 (1998)
52. Last I, Jortner J *J. Phys. Chem. A* **102** 9655 (1998)
53. Rose-Petruck C et al. *Phys. Rev. A* **55** 1182 (1997)
54. Bethe H, Salpeter E *Quantum Mechanics of One- and Two-Electron Atoms* (Berlin: Springer-Verlag, 1957) [Translated into Russian (Moscow: Fizmatgiz, 1960) Sect. 54]
55. Brunner W *Appl. Phys. B* **64** 443 (1997)
56. Ford J V et al. *J. Chem. Phys.* **110** 6257 (1999)
57. Neuman W *The Mechanism of Thermoemitting Arc Cathode* (Berlin: Akademie-Verlag, 1987)
58. Hoyaux M F *Arc Physics* (New York: Springer-Verlag, 1968)
59. Weidele H et al. *J. Chem. Phys.* **110** 8754 (1999)
60. Calvayrac F et al. *Eur. Phys. J. D* **4** 207 (1998)
61. Delone N B, Krainov V P *Multiphoton Processes in Atoms* 2nd ed. (Berlin: Springer, 2000)
62. Reinhard P G, Suraud E *Acad. Sci. Paris* **327** Ser. II b893 (1999)
63. Schlipper R et al. *Phys. Rev. Lett.* **80** 1194 (1998)
64. Tiggesbäumker J et al. *Chem. Phys. Lett.* **190** 42 (1992)
65. Bréchignac C et al. *Phys. Rev. Lett.* **70** 2036 (1993)
66. Haberland H et al. *Phys. Rev. Lett.* **69** 3212 (1992)
67. Haberland H et al. *Phys. Rev. Lett.* **77** 1415 (1996)
68. Smirnov B M *Usp. Fiz. Nauk* **167** 1169 (1997) [*Phys. Usp.* **40** 1117 (1997)]
69. Shao Y L et al. *Phys. Rev. Lett.* **77** 3343 (1996)
70. Sobel'man I I, Vaĭnshteĭn L A, Yukov E A *Vozbuzhdenie Atomov i Ushirenie Spektral'nykh Liniĭ* (Excitation of Atoms and Broadening of Spectral Lines) (Moscow: Nauka, 1979) [Translated into English (Heidelberg: Springer-Verlag, 1981)]
71. Brunner W, Ritze H H *Appl. Phys. B* **67** 47 (1998)
72. McPherson A et al. *Phys. Rev. Lett.* **72** 1810 (1994)
73. Ditmire T et al. *Appl. Phys. Lett.* **71** 166 (1997)
74. Ditmire T et al. *Phys. Rev. Lett.* **75** 3122 (1995)
75. Zweiback J, Ditmire T, Perry M D *Phys. Rev. A* **59** R3166 (1999)
76. Hu S X, Xu Z Z *Appl. Phys. Lett.* **71** 2605 (1997)
77. Véniard V, Taieb R, Maquet A *Phys. Rev. A* **60** 3952 (1999)
78. Donnelly et al. *Phys. Rev. Lett.* **76** 2472 (1996)
79. Tisch J W G et al. *J. Phys. B* **30** L709 (1997)
80. Reinhard P G, Suraud E *Eur. Phys. J. D* **3** 175 (1998)
81. Calvayrac F, Reinhard P G, Suraud E *J. Phys. B* **31** 1367 (1998)
82. Hora H *J. Opt. Soc. Am.* **65** 882 (1975)
83. Wickens L M, Allen J E *J. Plasma Phys.* **22** 167 (1979)
84. Last I, Jortner J *Phys. Rev. A* **60** 2215 (1999)
85. Brewczyk M et al. *Phys. Rev. Lett.* **80** 1857 (1998)
86. Brewczyk M, Rzazewski K *Phys. Rev. A* **60** 2285 (1999)
87. Poth L et al. *Chem. Phys.* **230** 309 (1998)
88. Springate E et al. *Phys. Rev. A* **61** 063201 (2000)
89. Ditmire T *Phys. Rev. A* **57** R4094 (1998)
90. Ditmire T et al. *Nature* (London) **398** 489 (1999)